Republic of Iraq
Ministry of Higher Education and Scientific Research
University of Al- Nahrain
College of Science

Simulation of Dose Buildup Factor of Gamma Ray Including Annihilation Radiation for Aluminum, Iron and Lead

A thesis

Submitted to the College of Science
University of Al-Nahrain
In partial Fulfillment of the Requirements for the
Degree of Master in Physics

By
Marwa Sabah Mahdi

(B.Sc.in Physics-2011)

SUPERVISORS

Dr. Laith A. Al-Ani ***Dr. Loay E. George***

Mars, 2014 **Jammada1, 1435**

بِسمِ اللهِ الرَّحمٰنِ الرّحِيَمِ

﴿ قَالُواْ سُبحَٰنَكَ لَا عِلمَ لَنَآ إِلَّا مَاعَلَّمتَنَآ إِنَكَ أَنتَ العَلِيمُ الحَكِيمُ ﴾

صدقَ اللهُ العَظيم

سورة البقرة

الاية (32)

الإهداء

إلى ربي .....الذي علم بالقلم علم الإنسان مالم يعلم

إلى الذي رباني صغيرا واقتديت به كبيرا..... أبي

إلى التي حملتني أملا وسقتني برعما..... أمي

إلى الشموع التي أنارت لي الطريق .....أختي وإخوتي

إلى أختي وأخي الذين لم تلدهم أمي..... علا وعلي

اهدي عملي هذا وفاءا وحبا لهم

مروة

Acknowledgement

I wish to express sincere gratitude to my supervisors, Dr. Laith A.Al-Ani and Dr. Loay E. George for their valuable guidance, patience and support, as well as giving me freedom during the preparation of my thesis and the chance to work under their supervision.

I wish to thank the head of Physics department Dr. Thaimr A.jumaa and the staff for their kind attention.

Deep thanks to Dr. Mouhammed Abud Alsaheb and to Mr. Adnan A. Abdulfattah and to Mr. Ammar Al-Rawi for help me in this work.

I would like to express my appreciate to my friends (Fala, Rasha and Mustafa), for help me in this work in one way or the other

Marwa

Supervisors Certification

I certify that this thesis entitled **"Simulation of Dose Buildup Factor of Gamma Ray Including Annihilation Radiation for Aluminum, Iron and Lead"** was prepared by **"Marwa Sabah Mahdi"** under my supervision at College of Science /Al-Nahrain University as a partial fulfillment of the requirements for the Degree of Master of Science /NuclearPhysics.

Signature:
Name: **Dr.Laith A. Al-Ani**
Title: Professor
Address: College of Science/ Al-Nahrain University
Date: / /2014

Signature:
Name: **Dr. Loay E. George**
Title: Assistant Professor
Address: College of Science / Baghdad University
Date: / /2014

In view of the available recommendation, I forward this thesis for debate by the examination committee.

Signature:
Name: Dr. Thamir A.Jabbar
Title: Assist. Professor
Date: / /2014

Examination Committee Certification

We certify that we have read this thesis entitled (**Simulation of Dose Buildup Factor of Gamma Ray Including Annihilation Radiation for Aluminum, Iron and Lead**) and, as an examining committee, examined the student (**Marwa Sabah Mahdi**) in its contents, it is adequate as a thesis for the degree of Master of Science in Nuclear Physics.

Signature:
Name: **Dr.Mazin M. Elias**
Title: Professor
Address: Al-Nahrain University
Date: / /2014
(Chairman)

Signature:
Name: **Dr.Khalid H.H. Al-attiyah**
Title: Professor
Address: College of Science/ Babylon Univesity
Date: / /2014
(Member)

Signature:
Name: **Dr.Asia H. Hammad**
Title: Assistant Professor
Address: College of Science/ Baghdad University
Date: / /2014
(Member)

Signature:
Name: **Dr.Laith A. Al-Ani**
Title: Professor
Address: College of Science/ Al-Nahrain University
Date: / /2014
(Member & supervisor)

Signature:
Name: **Dr. Loay E. George**
Title: Assistant Professor
Address: College of Science / Baghdad University
Date: / /2014
(Member & supervisor)

I, hereby certify upon the decision of the examining committee

Signature:
Name: **Dr. Hadi M. A. Abood**
Title: Assistant Professor
Address: Dean of the College of Science Al-Nahrain University
Date: / /2014

Abstract

A computer program based on Monte Carlo method had been designed and written in visual basic computer language and utilized for simulating the classic problem of gamma ray beam incident on finite plane slabs of absorbing materials. The source geometry adopted in this program is plane normal source.

Dose buildup factor of gamma photons in the absence and presence pair production effect have been calculated in the energy range (4-10) MeV for aluminum, iron, and lead up to 5 mean free path thickness.

Some of physical parameters has been studied and the simulation results indicates the following remarks:

- Gamma ray buildup factor increases with the increase of the thickness for the three shielding materials, this increase in dose buildup factor is due to the increase of scattering with the small angles and with the increase of the thickness of the material.
- Dose buildup factor for low atomic number material (Al, Z=13) is higher than that for medium (Fe, Z=26) and heavy (Pb, Z=82) material for the same photon energy (10MeV). A rapid decrease of the buildup factor values with the increase of Z is seen. This dependence is in a good agreement with the fact that the proportion of the cross section for Compton effect decreases with increasing atomic number, therefore the Compton effect plays a more significant role in lighter materials which have lower atomic number (Z).
- Dose buildup factor is inversely proportional with the increase of energy within the studied enrgy range (4-10)MeV. This behavior can be explained that the cross section for Compton scattering within the studied energy range is decreased with increase of

energy and this means that the probability of scattering is decreased and it is finally reflected on the buildup calculation, since the scattering plays an important role in determination of buildup factor.

The rate of increase in the value of dose buildup factor in lead (Z = 82) higher than iron (Z = 26), and the last is more than that for aluminium (Z = 13). This is due to the effect of pair production interaction which is directly proportional with the square of atomic number.

Dose buildup factor in the presence of pair production is higher than dose buildup factor in the absence of pair production effect. The deviation between the values of dose buildup factor in the presence and absence pair production is increased when the energy is increased within the studied energy; this mainly due to the increase of cross section for pair production values within the studied energy range.

List of Contents

Chapter Four
Summary, Conclusions and Suggestions

List of Figures

List of Tables

Chapter One
General Introduction

1.1 Introduction

Gamma rays have been identified in 1900 by Becquerel and Villard; they noticed that this kind of radiation had much higher penetrability than alpha and beta particles, it have short wavelength and high energy. Gamma rays have frequencies above 10 exahertz (or $<10^{19}$ Hz), and therefore have energies above 100keV and wavelengths less than 10 pico-meters (less than the diameter of an atom). They are classically produced by the decay from high energy states of atomic nuclei, when a nucleon is in a high energy orbit while a low energy orbit is unfilled; it can jump to the lower energy orbit with the energy thereby released coming off as a quantum of electromagnetic radiation, which we call a gamma ray.

The energy of photons is equal to the difference in energy levels between the two states involved in the transition. When there are two or more exited states are available, a cascade of photons occurs from the higher to intermediate stages then to the ground state. Photons are electrically neutral; therefore they do not steadily lose energy [Knol 00].

Gamma rays have high energies and high penetrating ability. Therefore, gamma rays is very dangerous for human cells and other living organisms when exposed in excessive dose, selection of shielding material becomes most important. Nuclear accidents due to natural and manmade disasters cannot be refused in future. People involved in industries, research laboratories and medical institutions may be victims of gamma ray exposure. For safety of these people, selection of shielding materials, becomes most important [Dhil 12].

1.2 Attenuation Law of Gamma Ray

Gamma ray passes through different materials, some of the photons interact with the particles of the matter and their energy can be absorbed or scattered. This absorption and scattering is called attenuation [Chil 84].

The absorbed dose of the worker in nuclear reactors obey to exponential decrease relation, that is: when gamma rays pass through a matter, the energy of ray will be decrease due to its interaction with matter.

The loss of gamma rays, or the reduction in the number of photon dN in a small thickness of matter dX at any point is proportional to the number of incident photons N:

$$dN \propto dX \text{ ; and } dN \propto N \tag{1.1}$$

The proportionality symbol can be replaced by a proportionality constant μ to become:

$$dN = -\mu N \, dX \tag{1.2}$$

The minus sign indicates that the number of photons decreases as the absorber thickness increases where μ is the attenuation coefficient and it is proportional to cross section σ:

$$\mu = N\sigma \tag{1.3}$$

where, N is the number of atoms in unit volume.

Equation (1.2) can also be written in terms of intensity

$$dI = -\mu \, I \, dX \tag{1.4}$$

If X is expressed as a length; then μ is called linear attenuation coefficient [m^{-1}].

When a photon is traversing a material in which the total linear attenuation coefficient is $\mu_{0,}$ then the distance $1/\mu_0$ (m) is called the mean

free path (mfp) which is defined as that the abscinded distance between two events [Al.An 89].

The mean free path is used in calculation to avoid the effect of density to different material.

By integrating equation (1.4), we obtain [Khan 84]:

$$I = I_0 e^{-\mu x} \qquad (1.5)$$

where I: the emerging intensity of gamma ray,

I_0: the incident intensity of gamma ray,

μ: attenuation coefficient (cm^{-1}),

x: thickness of absorber matter,

I/I_0: represents the gamma ray transmission.

This relation is correct only for narrow beam geometry.

1.3 Good Geometry and Poor Geometry

When gamma rays penetrate a material, the basic property of the gamma rays absorption in this material is the exponential decrease in the radiation intensity of a homogenous beam of gamma rays pass through a thin slab of matter, this decrease is determined from the relation (1.5). This decrease is valid only when the beam of gamma rays is narrow collimated beam; such geometry is called a "good" geometry.

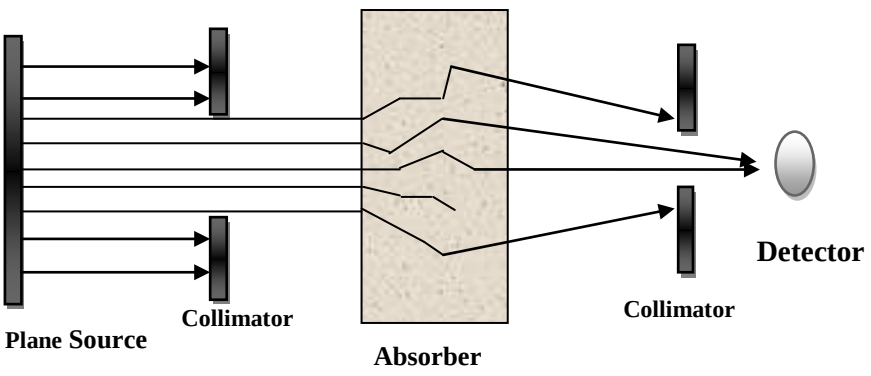

Fig (1.1) Good geometry

But, if the detector receives not only the direct attenuated beam but also some photons scattered from all points in the absorber with abroad beam the radiation intensity detected will be greater than that obtained under narrow beam is called a (poor geometry) as shown in figure (1.2), then equation (1.5) should adjusted to become [Evan 55]:

$$I = B\, I_o\, e^{-\mu x} \qquad (1.6)$$

where, B is the buildup factor; it can be considered as a simple correction factor which adjusts the result for the uncollided photons to include the contribution from the scattered and subsidiary radiation.

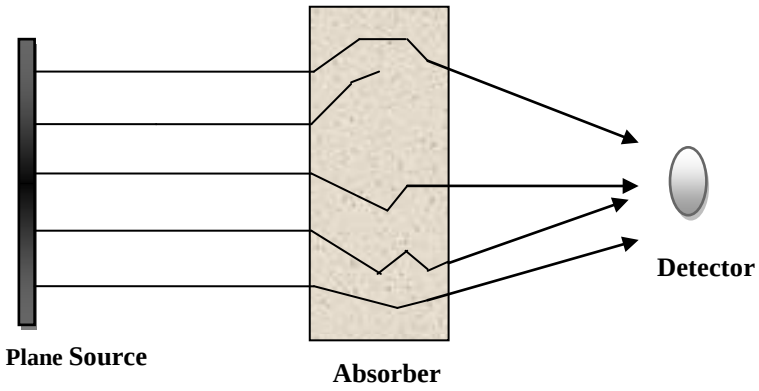

Fig (1.2) Poor geometry

1.4 Interaction of Gamma Rays with Matter

There are three main interaction mechanisms of photons with matter. They are: (i) Photoelectric effect, (ii) Compton scattering and (iii) Pair production. The predominant mode of interaction depends on the energy of the incident photons and the atomic number of the material with which they are interacting. At low energies, in high atomic number materials, the photoelectric effect is the main interaction of photons with the material. At intermediate energies in low atomic number materials the dominant interaction is Compton scattering. At very high energies, the main mechanism by which photons are detected is pair production (Kran 88).

1.4.1 Photoelectric absorption

In this process gamma ray may interact with abound atomic electron and it loses all of its energy and stopped to exist as a gamma ray. Some of the gamma ray energy is used to overcome the electron binding energy and most of the remainder energy is transferred to free electron as kinetic energy and a very small amount of recoil energy remains with the atom to conserve momentum.

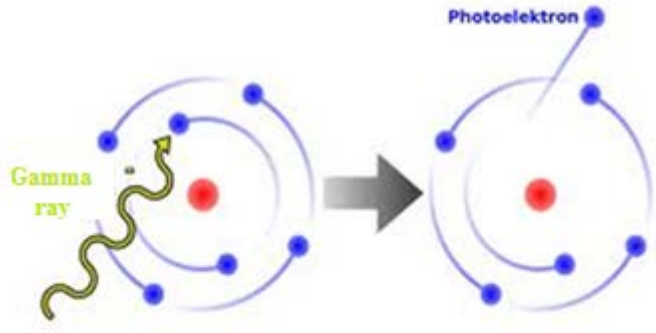

Fig (1.3) Illustration of the photoelectric absorption

The probability of photoelectric absorption depends on the atomic number of the atom and the electron binding energy and on the gamma ray energy [Chil 84]:

$$P = \frac{c\,Z^a}{(h\nu)^b} \qquad (1.7)$$

where, P is the probability, C: constant,

$$b = \begin{cases} 3 \; for \; h\nu < 0.5 \; MeV \\ 1 \; for \; h\nu \geq 0.5 \; MeV \end{cases}$$

The energy of free electron is given by:

$$E = h\nu - E_{Bind} \qquad (1.8)$$

where hν is the energy of gamma ray, E_{Bind} is the binding energy of electron.

Therefore the photoelectric effect absorption is appearing more in low photon energy and high atomic number materials [Evan 55].

1.4.2 Compton scattering

In Compton scattering gamma ray interacts with a free or weakly bound electron ($E_\gamma >> E_b$) and transfers part of its energy to the electron.

This interaction involves the outer, least tightly bound electrons in the scattering atom. The electron becomes a free electron with kinetic energy equal to the difference of the energy lost by the gamma ray and the electron binding energy. Because the electron binding energy is very small compared to the gamma ray energy, the kinetic energy of the electron is very nearly equal to the energy lost by the gamma ray [Evan 55].

$$E_e = E_\gamma - E^{'}$$

where E_e: energy of scattered electron, E_γ: energy of incident gamma ray, $E^{'}$: Energy of scattered gamma ray.

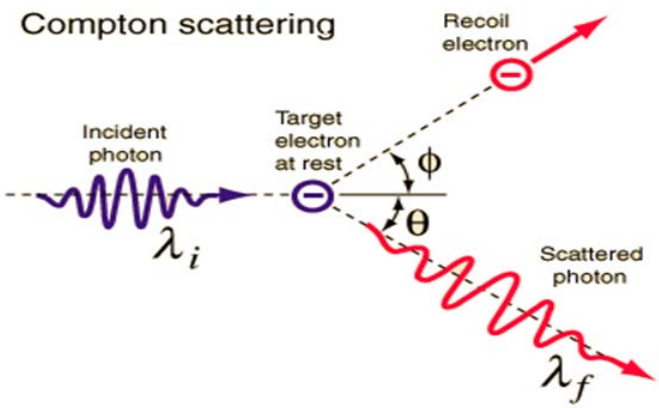

Fig (1.4) Illustration of Compton scattered

The energy of scattered photon is given by:

$$h\nu^{'} = \frac{h\nu}{1+[(1-cos\theta)h\nu/m_e c^2]} \qquad (1.9)$$

hν: energy of incident photon,

θ: scattered angle of photon.

And, the energy of scattered electron is given by:

$$E = h\nu\left[\frac{(1-cos\theta)h\nu/m_oc^2}{(1+cos\theta)h\nu/m_oc^2}\right] \quad (1.10)$$

Because Compton scattering involves the least tightly bound electrons, the nucleus has only a minor influence and the probability for interaction is nearly independent of atomic number. The interaction probability depends on the electron density, which is proportional to $\frac{Z}{A}$ and nearly constant for all material except hydrogen [Knol 79].

1.4.3 Pair production

This interaction has a threshold of 1.022 MeV because it is the minimum energy required to create the electron and positron. If the gamma ray energy exceeds 1.022 MeV, the excess energy is shared between the electron and positron as kinetic energy. This interaction process is relatively unimportant for nuclear material as say because the most important gamma ray signatures are below 1.022 MeV [Evan 55].
The probability of pair production is given by:

$$P = N\,Z^2\,f(E,Z) \quad (1.11)$$

where, $f(E,Z)$is a function depends on E and Z.

Z atomic number

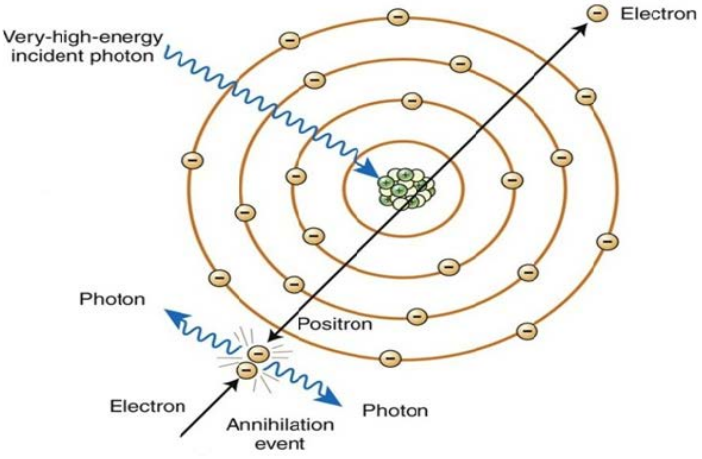

Fig (1.5) An illustration of the pair production

Pair production cross sections are usually expressed in units of the quantity:

$$\sigma = \sigma_0 Z^2 \left(\frac{28}{9} \ln\left(\frac{2E}{m_0 c^2}\right) - \frac{218}{27}\right) \qquad (1.12)$$

$$\sigma_0 = 5.8e^{-28} \quad \frac{\text{cm}^2}{\text{nucleus}}$$

The cross section is zero for photons energies less than 1.02 MeV, while for greater energies; it increases at first slowly, then more rapidly. This increase is proportional to Z^2 so that for a given photon energy, pair production increases quite rapidly with atomic number [Kapl 77].

Beside the above mentioned three major processes, minor processes may occur when gamma rays interact with matter as [Meye 67]:

1. Coherent electrons scattering (Rayleigh scattering),
2. Annihilation ray,
3. Fluorescence ray,
4. Bremsstrahlung ray,
5. Thomson scattering from nuclear,
6. Crystal scattering,
7. Nuclear reactions.

1.5 Buildup Factor

Buildup factor can be defined as the ratio of the detector response to the radiation at the point of interest to the detector response to the uncollided radiation at the same point. Build up factor expressed in different quantities [Gold 54]:

1. The number buildup factor B_N is defined as :

$$B_N = \frac{\int N_t \, dE}{\int N_{uns} \, dE} \qquad (1.13)$$

where, N_t: total number of photons reached to detector,

N_{uns}: number of unscattered photons reached to the detector.

2. The energy buildup factor B_E is defined as:

$$B_E = \frac{\int E_t \, dE}{\int E_{uns} \, dE} \quad (1.14)$$

where, E_t: total energy of photons reached to detector,

E_{uns}: energy of unscattered photon reached to detector.

3. The dose buildup factor B_D is defined as:

$$B_D = \frac{\int \mu_{air} \, E_t \, dE}{\int \mu_{air} \, E_{uns} \, dE} \quad (1.15)$$

where, μ_{air} is the energy absorption coefficient of air.

Buildup factor depends on [Wood 81]:

1. The distance of penetration through the attenuating medium.
2. The type of medium expressed in terms of atomic charge number Z for elemental materials.
3. The energy of the source photons, and their direction of emission.
4. The geometric configuration of the attenuating medium and the geometry of the source.
5. The position of source and detector and the main incident angle on the shield.
6. The distance between detector and collimator.

1.6 Types of Gamma Shields

The gamma shields may be classified into two types:

1. Single layer shields:

a. Pure single shields: this type of shields composed of one pure element as (Aluminum, Iron and Lead).

b. Homogeneous mixture: This shields used as saving shields from gamma ray, it is consist of alloys homogeneous mixture, depends on effect atomic number Z_{eff}, that given by:

$$Z_{eff} = \frac{\sum W_k Z_k^2 / A_k}{\sum W_k Z_k / A_k} \quad (1.16)$$

where: W_k: molecule weight to element K in the homogeneous,

A_k: atomic weight to element K.

2. Multi- layer shields:

The value of gamma rays buildup factor is different when the shield is multi layer from the single layer shields. Some of reactor shields require the shield to be multi-layer shields to different materials and the buildup factor is taken varied values according to the layer that penetrated previously [Wood 81].

1.7 Calculation Methods of Buildup Factor

The calculation method of buildup factor can be divided into three groups [Chil 84]:

1- Analytical methods.
2- Empirical formula based methods.
3- Statistical calculation based methods.

1.7.1 Analytical method

The calculation of buildup factor analytically can be performed by solving Boltzman transport equation. Due to the complex buildup dependency, the analytical expressions of buildup factor are still based on empirical description of the measured or calculated curves [Wood 81].

1.7.2 Empirical formula

In the calculation involving buildup factor it is convenient to have mathematical expression for B. Some of the most commonly used formula are [Chil 84]

i- For a single layer shields:

a- Linear formula [Wood 81]

$$B = 1 + K(\mu x) \tag{1.17}$$

where: K is a constant and calculated as follows:

$$K = B(1) - 1$$

(1.18) μ: linear attenuation coefficient for the shield material,

x: shield thickness in cm,

μx: shield thickness in mean free path (mfp).

b- Taylor formula

For a point isotropic source in infinite medium, the buildup factor is defined as [Chil 84]:

$$B = A\, e^{(-\alpha_1 \mu r)} + (1 - A) e^{(-\alpha_2 \mu r)} \qquad (1.19)$$

The coefficients values of A, α_1, α_2 are found in [Wood 81], they published for many materials.

The importance of this equation comes from its simplicity; therefore it is adopted in a wide range of applications.

c- Berger formula

This formula strikes a good balance between accuracy and computing complexity [Chil 80]:

$$B(\mu x) = 1 + a\, \mu r\, e^{(b \mu r)} \qquad (1.20)$$

where, a & b are the parameters depends on function of the source, photon energy and attenuating medium.

d- Capo formula

In this formula, the buildup factor is given by:

$$B(E_o, \mu x) = \sum_{i=0}^{3} B_i\, (\mu x)^i \qquad (1.21)$$

where: $B_i = \sum_{j=0}^{4} C_{ij} \left(\frac{1}{E}\right)^j$

The coefficient C_{ij} is found in [Capo 58].

***ii.* For multi-layered shields:**

Also, there are many methods have been noticed in the literature, among them are the following

a- Coldstein method of an effective atomic number: This method propose the homogenization of the shield layers by specifying a single effective atomic number Z for the shield. The buildup factor for the composite shield then depends on the actual number of mfp's penetrated by the radiation and on Z [Wood 81].

b- Blizared method: In this method the atomic number Z, of the last material penetrated by the radiation is taken. Also, the total attenuation thickness of the shield, $(\sum_i \mu i\ xi)$ is taken as the argument is entering the basic buildup factor tables. This method should not be used if the last layer is less than 3 mfp in thickness [Wood 81].

c- Broder formula: It is a more refined approach to the multi-layer problem Broder.

Here an attempt is made to allow for the passage of the photons through the previous layer, by assuming the buildup contribution of each layer is additive and can be found as a result of a simple differencing procedure [Brod 62]:

$$B = \sum_{n=1}^{N} B_n \left(\sum_{i=1}^{n} X_i\right) - \sum_{n=2}^{N} B_n \left(\sum_{i=1}^{n-1} X_i\right) \qquad (1.22)$$

where X_i is the layer thickness in mfp, B_n is the dose buildup factor for N layers with thickness X_i.

d- Kalos Method: Kalos at 1980, studied the buildup factor for a shield consisting of two layers (water and lead). He found that when a layer of lead was put behind a water layer, it would reject the low-energetic, scattered and transmitted photons from the water layer. Whereas if a

layer of water was put behind a lead layer, the rejection of the low – energetic photons will decrease. Therefore, the value of build up factor in the second case should be higher than its value in the first case. The buildup factor was calculated by Kalos and the calculations led to the following two simi-imprical formulas [Jian 80]:

1) For lead followed by water, $0.5 \leq E \leq 10$ MeV, the buildup factor is:

$$B(x_1, x_2) = B_2(x_2) + \frac{B_1(x_1) - 1}{B_2(x_1) - 1} \times [B_2(x_1 + x_2) - B_2(x_2)] \quad (1.23)$$

where;

- B(x_1, x_2) is the buildup factor for the two layers.
- $B_2(x_2)$ is the buildup factor of the second layer (water) at a thickness x_2 in mfp unit.
- B_1 (x_1) is the buildup factor of the first layer (lead) at a thickness x_1 in mfp.
- $B_2(x_1)$ is the buildup factor of the second layer at a thickness x_1 in mfp unit.

2) For water followed by lead, 0.5≤ E ≤ 10 MeV, the buildup factor is:

$$B(x_1, x_2) = B_2(x_2) + \left[\frac{B_1(x_1)}{B_2(x_1)} \exp(-1.7x_2) + \frac{(\mu_c/\mu_t)_1}{(\mu_c/\mu_t)_2} \times (1 - \exp(x_2)) \right] \times [B_2(x_1 + x_2) - B_2(x_2)] \quad (1.24)$$

where;

- B(x_1, x_2) is the buildup factor for the two layers.
- $B_2(x_2)$ is the buildup factor for the second layer (lead) at a thickness (x_1) in (mfp) unit.
- $B_1(x_1)$ is the buildup factor of the first layer (water)at a thickness (x_1) in (mfp) unit.
- $B_2(x_1 + x_2)$ is the buildup factor of the second layer at the summation of the thicknesses (x_1) and (x_2).

$\frac{(\mu_c/\mu_t)_1}{(\mu_c/\mu_{t_2})}$ is the ratio between Compton scattering attenuation coefficient and the total attenuation coefficient for the first layer to its ratio for the second layer.

1.7.3 Statistical calculation (Monte Carlo Method)

The Monte Carlo method has been proven to be a powerful and versatile tool in solving particle transport problems that are difficult or impossible to solve adequately by other mathematical techniques.

The basic form of this method is simulating the actual physical processes which govern the real particle's behavior. The epithet Monte Carlo arises from the use of random numbers to determine the outcome of a sequence of chance events [Robi 81].

The basic idea of Monte Carlo is to create a series of life histories of the source particles by using random number sampling techniques to sample the probability laws that describe the real particle's behavior and to trace out the particles random number movement through the medium. The history of a particle is traced until it can no longer contribute information of interest to the problem in hand. The life history is then terminated and a new particle is started from the source [Wood 81]. The detailing of this method explained in chapter two of this thesis.

In considering Monte Carlo Method one can usefully distinguish between two main forms:

i. The basic or analogue in which the sampling procedures used are straight forward and the schematization followed closely resembles the actual physical processes, in this form there is a strong analogy between the physical particles and the mathematical particles followed by the computer.

ii. The more sophisticated approach (non-analogue), in which the game played is modified to improve statistical efficiency, and hence for a

given computing effort a reduction is achieved in the error of the Monte Carlo estimation of the mean.

Monte Carlo methods vary, but tend to follow a particular pattern:

1. Define a domain of possible inputs.
2. Generate inputs randomly from a probability distribution over the domain.
3. Perform a deterministic computation on the inputs.
4. Aggregate the results.

1.8 Literature Survey

The literature from 1950 on gamma rays buildup factors using different radiation sources and different media was surveyed. Many of these studies were treated and processed by Monte Carlo calculation. The interest in the buildup factor started in the early of 1950, when the first study including its measurement had been published. Because of the depending of buildup factor on many factors, the nature of studies varied. The published studies can be classified as following:

1.8.1 Experimental method

In 1950, G.R. White started a first study for the buildup factor for water. She used the ^{60}Co source with two types of detectors (G.M. tube and ionization chamber) where the results appeared that the buildup factor increased exponentially with increasing the thickness of the layer of the water that used in measurement, and the buildup factor value of thickness 46 cm of water was 4.51[Whit 50].

Burke and Beck, in 1974, have measured dose buildup factor for normally incident 0.662 MeV gamma rays penetrating lead slab, they also calculated buildup factors from normally incident (662 KeV) gamma rays penetrating multi-layer Aluminum-lead slabs for various combinations using thermo luminescence dosimeters. Their results were compared with

calculated values obtained from a gamma rays transport code and with values inferred from a Simi empirical formula using single layer slab buildup factor [Burk 74].

Bishop in 1987, presented a measurement for buildup factor of energies 1.43 MeV, 2.75 MeV and 6.13 MeV where the resulted spectrum from analyzing the slabs of concrete, lead and iron was investing by using NaI (TI) detector [Bish 87].

In 1989 Al-Ani had made an investigation of buildup factor calculation on Fe, Cu, Al, and concrete using two radioactive sources ^{60}Co and ^{137}Cs and he depended in his research, he investigated the effect of geometrical factor on the buildup factor in addition to the effect of detector type [Al-An 89].

In 1994 Hattif had measured the buildup factor for aluminum, iron, copper, brass, and lead by using the ^{137}Cs and ^{60}Co energy sources with NaI (TI) detector [Hatt 94].

2. Theoretical method/ Monte Carlo Method

Morris and Chilton in 1970 calculated the buildup factor for the water using two different methods (Monte Carlo and moment) with two point sources of energies, respectively (0.5 and 1 MeV) [Morr 70].The discrepancy between the results of these methods was less than 5%.

In 1987, Hirayama presented a comparison of gamma rays buildup factors for low Z material and for low energies using discrete ordinates and point Monte Carlo method. He calculated the exposure and absorbed dose buildup factor for a point source in an infinite Beryllium in the low energy range of 0.03 to 0.3 MeV for penetration depth up to 40 mfp. He used three discrete ordinates codes; (PALLAS-PL, SP-Br and ANISN).

The study showed a reasonable agreement with the results obtained by point Monte Carlo calculations using the "electron gamma shower version (4) code". He found that for both methods the results up to 10 mfp were in good agreement for point sources with those of the EGS4 as a test standard by the point Monte Carlo method. Also, the study showed a fairly good agreement of the values of the buildup factors for Beryllium by PALLAS and ANISN [Hira 87].

In 1988, Herbold investigated a Monte Carlo calculation of energy buildup factors in the range from 15 KeV to 100 KeV, with special reference to the ^{125}I dosimeter. Dose buildup factors of point isotropic gamma sources in water were calculated based on the formalism given by M.Berger and using the Monte Carlo code EGS4. This study included all effect of penetration, specially electron transport and Rayleigh scattering. It was found that the new buildup factors show considerable deviation relative to Berger's formula [Herb 88].

Al-Samaraey, in 2002, had presented a study about the calculation of gamma rays buildup factor for the conical beam using Monte Carlo method for three different materials aluminum, iron, and lead. The number buildup factor from ^{137}Cs and ^{60}Co was calculated by using Monte Carlo method. As a conclusion from his investigation, the using of theoretical as an input data programs of gamma rays calculation instead of these experimental one which are usually used in the buildup factor calculation [Al-Sa 02].

In 2003, Al-Rawi used Monte Carlo method to calculate buildup factor for two materials, water and lead, he used two radioactive sources, ^{60}Co and ^{137}Cs, he depended in his research upon the effect of energy, thickness, and atomic number on buildup factor [Al-Ra 03].

3. Theoretical Method/ Moment method

In 1975, Eisenhower and Simmon presented a theoretical study about the energetic buildup factor calculation, absorbed energy and dose for concrete in accordance of that source was a point and symmetric with energy range from 0.015 to 15 MeV, using the moment method. They concluded that the buildup factor with the exist are of inhalation radiation is higher than that without it [Eise 75].

Morris et al, in 1975, had presented a measurement for buildup factor for energy deposition in water and aluminum and for exposure in concrete for monoenergetic, isotropic point gamma ray sources. The buildup factor were evaluated using the method of moments and are tabulated for energies from 0.03 to 10 MeV, and distance out to 50 mfp from the source. Empirical representations of these buildup factors are developed using Berger's formula. Fitting parameters are tabulated for each material as a function of source energy [Morr 75].

In 1980, Chilton et al calculated the buildup factor for photons of point isotropic source in infinite homogeneous samples of air, water and iron by moment's method code. Then the results gives the parameters in the Berger empirical formula for buildup factors have been evaluated. The Berger formula was shown to fit the calculational results for nuclei of low atomic number at energies above 1 MeV and below 0.06 MeV. In mid energy range, differences of as much as 40% are observed. The concrete buildup factor data have been fitted to both the Taylor and the Berger empirical formulae [Chil 80].

Also, in the year 2001 Al-Baiti had measured the buildup factor for single and multi-layer shield for aluminum, iron, copper, brass, and lead

materials. He calculated the buildup factor by using the moment method with the information of the linear formula. He used Kalos method for calculating the buildup factor for double layers shield [Al-Ba 01].

In 1963, Hubbel investigated and formulated a buildup factor form using a power series technique. He evaluated the response of an isotropic detector to primary radiation from a finite plane source as the sum over an infinite series. This study was investigated as an application to rectangular and off–axis disk source problem [Hubb 63].

Metghalchi, in 1978, had determined the coefficients of Berger's formula for gamma rays buildup factor in ordinary concrete, his work showed that the coefficients available for Taylor formula has improved considerably. He depended on the Chilton's conclusion which illustrate that "the accuracy that can be achieved using fitted values of two parameters is better in general than previously suggested formulas of three parameters or less" [Metg 78].

In 1981, Foderaro and Hall, suggested a new formulation for fitting the results of buildup factor because of the high relative standard deviation for the Taylor and Berger formula when thickness is increased. This new formula was called "the three-exponential representation"; its fit for the buildup factor data of water was better than either of the Berger or the Taylor representation [Fode 81].

Monte Carlo method (code RADAK) was used by Bishop in 1987 to calculate the exposure buildup factor for source of energy 2.75 MeV in the double layer shielding of lead iron and aluminum. He showed that for double layer shield, the increase of buildup factor values when using a material of low atomic number in the beginning following it a material of

height atomic number, is differ from using just a material of low atomic number with the same thickness by the (mfp) units [Bish 87].

In 1989, a study of gamma rays buildup factors for a point isotropic source in stratified spherical shields was presented by "Min-Fungus and Shaing-Huei Jiang". It was a general review of investigations of gamma rays buildup factors. They used for this study the one-dimensional gamma rays transport code BIGGI-4T. The authors concluded that in the calculation of stratified shields with a special adjustment (constant μ_0) the density variation effect could be eliminated [Fong 89].

Bakos in 1994 presented a study of buildup factors for energies 1.6, 6.13 and 7.10 MeV photon penetration through multiple layer shielding slabs. Theoretical and experimental calculation of dose was determined for penetrations through various thicknesses of aluminum (Al), steel (Fe), and lead (Pb). He concluded that in the case where lead forms the outer layer, the buildup factor is reduced. Whereas when steel forms the outer layer the dose buildup factor approached the buildup factor of an all steel shield of the same total mfp penetration [Bako 94].

Al-Amaar, in 1996, measured and studied the angular distribution for the buildup factor for the single and double layer of iron by using energy source Co-60 and NaI (TI) detector. His results appeared in accordance with the theoretical and experimental international published results for the single and double layer of the buildup factor [Al-Am 96].

In 1998, Kadotani and Chimizu presented an investigation of buildup factor and the energy and angle dependent doubly differential gamma rays albedo for homogenous semi–infinite medium for (water, ordinary concrete, soil, heavy concrete, iron, tin and lead), the invariant impeding method was the procedure of calculation employed in this

study, which has developed to solve the natural particle transport problems in homogenous one dimensional medium. The accuracy of the calculated gamma rays albedo was ascertained by comparing with the Monte Carlo calculations (MCNP4A and EGS4). From this study they produced a new energy and angle dependent differential gamma rays albedo database for several shielding material using the invariant embedding method [Kado 98].

Shimizu in 2000 presented an article described the development of a new semi-analytical method for radiation transport problems in slabs called "angular eigen value method and its application to the penetration of gamma rays in slabs". According to this method, an exact solution of energy and angular distribution of transmitted radiation in a slab can be obtained; based on the multi group approximation for energy and the discrete approximation for angular variable. His method is characterized by its application to the deep penetration of radiation more easily than other dependable methods, since a solution was expressed analytically as a function of the slab thickness. The calculation was made on the buildup factor of concrete slabs for plane oblique sources. It was concluded that the presented method could provide solutions with accuracy comparable with other dependable methods such as the Monte Carlo and moment method [Shim 00].

The same author in 2002 [Shim 00] developed a method of angular eigen value for deep penetration problems of gamma rays, as a new semi-analytical method for radiation transport problems in slabs. He calculated the exposure buildup factors for concrete slabs under slant incidence conditions by the presented method, and they were found in good agreement with Monte Carlo calculations by Fourine and Chilton up to the thickness of 10 mfp. He found throughout his study that the angular

eigen value method could provide solutions with accuracy comparable with dependable method.

Makki in 2009 measured the buildup factor for double layers shield (water and lead) using the source energy ^{137}Cs and ^{60}Co, she is found that the buildup factor increase with the increase of the total thickness of the shield. For three layers shield, the value of buildup factors approximates rapidly that of the outer material. Buildup factor for Water followed Lead shield is higher than that for Lead followed by Water for the same thicknesses [Makk 09].

In 2009 Sardari et al, have computed buildup factor of gamma- and X-ray photons in the energy range 0.2–2 MeV in water and soft tissue using Monte Carlo method. The results are compared with the existing buildup factor data of pure water. They found that the Buildup factor for water obtained by Monte Carlo as a whole is smaller than the values given in the literature, this is specifically true for μr>4. For small μr the difference is less than 4% and for larger μr would be up to 15%. For the case of μr<2, the results of Monte Carlo is usually higher than the literature. For μr>7 water buildup factor is lower than soft tissue. For μr<4 is vice versa. For high energy photons, and μr<2, buildup factor of water is greater than that of soft tissue [Sard 09].

In 2010 Manohara et al, computed gamma ray energy-absorption buildup factors using the five-parameter geometric progression (G-P) fitting formula for seven thermoluminescent dosimetric (TLD) materials in the energy range 0.015–15 MeV, and for penetration depths up to 40 mfp. They concluded that the effective atomic number, Z_{eff}, of BeO and LiF matches with that of cortical bone, and hence these compounds may be used as tissue equivalent materials for cortical bone in the energy

range 0.2–2 MeV. BeO and $Li_2B_4O_7$ can be used as tissue equivalent materials for breast tissue in the low energy region 1–8 keV and 1–10 keV, respectively [Mano 10].

In 2011, Alamatsaz and Mokari they studied the gamma exposure buildup factors (E.B.F.) for plane sources and two-layer shields of water and lead were calculated. Also, coherent scattering effect usually left unattended in this type of geometry and application was considered. First, gamma EBFs were calculated by using MCNP code, without considering coherent scattering effect for a normal and anisotropic plane source and double stratified layers of water-lead and lead-water. Then, the above mentioned factors were calculated by considering coherent scattering effect, and influence of coherent scattering and also fluorescence radiations on E.B.F. was studied. Due to coherent scattering, EBFs were increased in both layers, especially for sources with low energies and layers with more mean free paths. Regarding the high accuracy of statistical calculation and the applied cross sections, more complete results in comparison with previous works for the mentioned geometry were obtained [Alam 11].

In 2012, Singh et al, they studied the exposure buildup factor for some flyashes like Bitum inous, Subbituminous, lignite, high calcium, high iron, low calcium, and low iron has been calculated in the energy region 0.015-15.0 MeV up to a penetration depth of 40 mfp. The five G.P. fitting parameters have been used to calculate EBF. Variation of EBF with incident photon energy and penetration depth has been studied. It has been observed that chosen flyash have maximum value of EBF at 0.3 MeV. Variation in value of EBF is due to dominance of different interaction processes in different energy regions. Comparison of calculated exposure buildup factor with standard shows good agreements.

This study of buildup factor of Flyash will be helpful in estimating the transport and degradation of gamma radiations in these flyashes. Mostly Lead and Mercury are used as shielding materials. But these are difficult to use at large scale due to their higher cost and availability. Flyash can be used as a gamma-ray shielding material in field experiments which is suitable from the point of view of cost and availability [Sing 12].

Ochbelagh and Aziimkhani, in 2012, have used concrete mixed with different percentages of lead to study gamma-ray shielding properties. The transmitted fluxes of gamma-rays that were emitted from ^{137}Cs and ^{60}Co sources were detected by a NaI(Tl) detector and analyzed by a MCA analyzer. Then, the linear attenuation coefficients and compressive strength of concrete specimens were experimentally investigated. They compared the obtained data from concrete specimens with and without lead, and observed that; if the powder of lead to cement ratio of 90% by weight is added in the concrete mixture, the concrete can be used as a suitable shield against gamma rays [Ochb 12].

Shirani and Alamatsaz in 2013, calculated the exposure buildup factors by Monte Carlo method for point isotropic gamma ray sources, penetrating a two-layer spherical shield of water surrounded by lead. The buildup factors were then calculated for various combinations of water and lead layers at some gamma ray energy points in the range from 0.04 MeV to 10 MeV and for shield thicknesses from 1 to 10 mean free paths (mfp), they conclude that at low gamma ray energies (E_γ <0.5 MeV) where photoelectric effect is dominant, the best combination is zero mfp water -10 mfp lead (lead alone), at intermediate energies (1 MeV< E_γ <3 MeV) where Compton scattering is dominant 5 mfp water-5 mfp lead (half water-half lead) could be taken as optimum combination, and finally

at E_γ =10 MeV where bremsstrahlung is dominant in lead the best combination is 10 mfp water- zero mfp lead (water alone) [Shir 13].

1.9 Aim of This Work

Buildup factor represents an important correction factor in the calculation process of building factor of the shields of nuclear reactors. It is interesting issue in health physics and in shielding the research laboratory.

The aim of the present work is to study a gamma ray build up factor in the absence and presence of the effect of pair production interaction for a single finite planer shielding materials, and for different values of atomic number and for plane normal source with different energy values.

To a chief the study target a computer program will be designed and build for simulating the classical problem of gamma beam based on Monte Carlo method.

Chapter Two

Theory

2.1 Introduction

When studying gamma rays buildup factor, it is better to use theoretical method because, in many cases, experimental studies of gamma rays buildup factor face many difficulties; highly active sources are needed and the absorber thickness are limited to no more than a few mean free paths, under such circumstances the researchers may be at the risk of exposure to a high ionizing gamma radiation. For these reasons, it is better to use theoretical tools which enable researchers to study in details gamma rays buildup factor. One of the important tools is Monte Carlo method, which is a method of computer simulation of a system with many degrees of freedom. Its name is derived from the use of random numbers to simulate statistical fluctuations in order to numerically generate probability distributions. An effective and economic use of this method requires the use of high speed digital computers. The specific advantage of Monte Carlo computer experiment is that it yields information on model system which in principle is numerically exact. Another advantage obtained macroscopic information on the system both in space and in time. This information can be much more detailed than what is available from experiments on real system [Bind 79].

In this chapter, the theoretical background of this method is described first, and then a detailed explanation of the program used to calculate buildup factor by Monte Carlo method is presented.

2.2 The Monte Carlo Method

Monte Carlo means using random numbers in scientific computing. More precisely, it means using random numbers as a tool to compute something that is not random.

The basic idea of Monte Carlo is to create a series of life histories of the source particles by using random number sampling techniques to sample the probability laws that describe the real particle's behavior and to trace out the particles random number movement through the medium.

Simulation means producing random variables with a certain distribution just to look at them. For example, we might have a model of a random process that produces clouds. We could simulate the model to generate cloud pictures, either out of scientific interest or for computer graphics. As soon as we start asking quantitative questions about, say, the average size of a cloud or the probability that it will rain, we move from pure simulation to Monte Carlo.

Monte Carlo simulation is a computerized mathematical technique that allows people to account for risk in quantitative analysis and decision making. The technique is used by professionals in such widely disparate fields as finance, project management, energy, manufacturing, engineering, research and development, insurance, transportation, and the environment. Monte Carlo simulation furnishes the user with a range of possible outcomes and the probabilities they will occur for any choice of action. It shows the extreme possibilities the outcomes of going for broke and for the most conservative decision along with all possible consequences for middle of the road decisions [Rubi 81].

Historically, the name and the systematic development of Monte Carlo methods can be traced back to 1944. The real use of Monte Carlo methods as a research tool stems from work on the atomic bomb during the Second World War. This work involved a direct simulation of the

probabilistic problems concerned with random neutron diffusion in fissile material [Hamm 64].

2.2.1 The work essentials of Monte Carlo

Monte Carlo simulation performs risk analysis by building models of possible results by substituting a range of values based on the probability distribution for any factor that has inherent uncertainty. Then, it calculates results over and over; each time using a different set of random values obey to certain probability functions. Depending upon the number of uncertainties and the ranges specified for them, a simulation based on Monte Carlo could involve thousands or tens of thousands of recalculations before it is complete. Monte Carlo simulation produces distributions of possible outcome values [Nayl 66].

By using probability distributions, variables can have different probabilities of different outcomes occurring. Probability distributions are a much more realistic way of describing uncertainty in variables of a risk analysis. Common probability distributions include:

1- Normal: Or “bell curve” The user simply defines the mean or expected value and a standard deviation to describe the variation about the mean. Values in the middle near the mean are most likely to occur. It is symmetric and describes many natural phenomena such as people’s heights. Examples of variables described by normal distributions include inflation rates and energy prices.

2- Log-normal: Values are positively skewed, not symmetric like a normal distribution. It is used to represent values that don’t go below zero but have unlimited positive potential. Examples of variables described by lognormal distributions include real estate property values, stock prices, and oil reserves.

3- Uniform: All values have an equal chance of occurring, and the user simply defines the minimum and maximum. Examples of variables that could be uniformly distributed include manufacturing costs or future sales revenues for a new product.
4- Triangular: The user defines the minimum, most likely, and maximum values. Values around the most likely are more likely to occur. Variables that could be described by a triangular distribution include past sales history per unit of time and inventory levels.
5- PERT: The user defines the minimum, most likely, and maximum values, just like the triangular distribution. Values around the most likely are more likely to occur. However values between the most likely and extremes are more likely to occur than the triangular; that is, the extremes are not as emphasized. An example of the use of a PERT distribution is to describe the duration of a task in a project management model.
6- Discrete: The user defines specific values that may occur and the likelihood of each. An example might be the results of a lawsuit: 20% chance of positive verdict, 30% change of negative verdict, 40% chance of settlement, and 10% chance of mistrial [Bhat 67].

Monte Carlo simulation provides a number of advantages over deterministic:

- Probabilistic Results: The results show not only what could happen, but how likely each outcome is.
- Graphical Results. Because of the data a Monte Carlo simulation generates, it is easy to create graphs of different outcomes and their chances of occurrence. This is important for communicating findings to other stakeholders.

- Sensitivity Analysis. With just a few cases, deterministic analysis makes it difficult to see which variables impact the outcome the most. In Monte Carlo simulation, it is easy to see which inputs had the biggest effect on bottom-line results.
- Scenario Analysis: In deterministic models, it is very difficult to model different combinations of values for different inputs to see the effects of truly different scenarios. Using Monte Carlo simulation, analysts can see exactly which inputs had which values together when certain outcomes occurred. This is invaluable for pursuing further analysis.
- Correlation of Inputs. In Monte Carlo simulation, it is possible to model interdependent relationships between input variables. It's important for accuracy to represent how, in reality, when some factors go up, others go up or down accordingly.

2.2.2 Major Components of a Monte Carlo Algorithm

The major components of Monte Carlo method comprise the foundation of most Monte Carlo applications. An understanding of these major components will provide a sound foundation for the reader to construct his own Monte Carlo method. The primary components of a Monte Carlo simulation method include the following [Span 69]:

1. Probability distribution functions (pdf's): the physical system must be described by a set of pdfs (probability distribution function).
2. Random number generator: a source of random numbers uniformly distributed on the unit interval must be available.
3. Sampling rule: a prescription for sampling from the specific pdfs assuming the availability of random numbers on the unit interval must be available.

4. Scoring (or tally): the outcomes must be accumulated into overall tallies or scores for the quantities of interest.
5. Error Estimation: an estimate of the statistical error (variance) as a function of the number of trials and other quantities of interest.
6. Variance Reduction Techniques: are methods for reducing the variance of the estimated solution, or reduce the computational time for Monte Carlo simulation.
7. Parallelization and Vectorization: are algorithms to allow Monte Carlo method to implemented efficiency on advance computer architectures.

2.3 Particle Trajectory

When Monte Carlo method is used, the particles histories are generated by simulating the random nature of the particles interactions with medium. Life history of a particle is built up from acknowledge of its trajectory through the particular system of interest. Consider the path of the particle as it travels through some homogenous medium. Since the typical particle scatters frequently the path is zig-zag rather in the manner indicated in the figure (2.1). Here the particle originates at A with known direction and energy. It has a free flight until it has a collision with an atom of the medium. This collision could result in the absorption of the particle and the immediate termination of its history, but it is assumed to be scattering interactions and the particle continues with a new direction and the change of energy (or wavelength). This change of energy and direction is a statistical process which mean that no unique energy and direction after a scattering; rather, there is a probability distribution for each of these variables. After the first scattering the same particle makes another free flight and experiences another collision and so on.

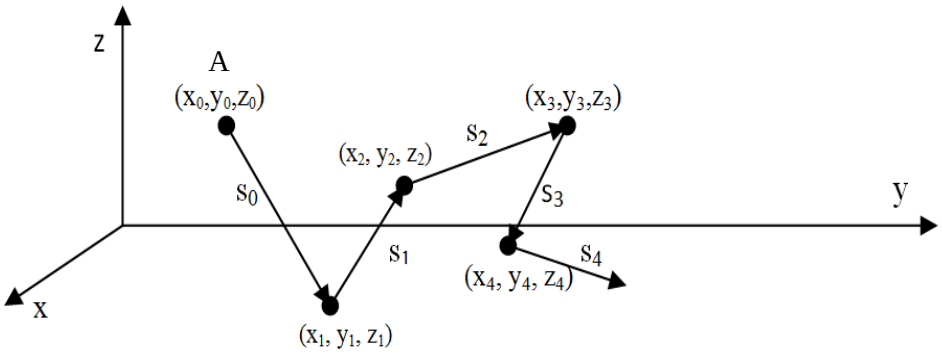

Fig (2.1) A typical particle's "random walk" through a medium [Wood 81]

In order to track the particle during its journey it is necessary to know: its spatial coordinates (x, y, z), the spherical coordinates $(\theta, \emptyset)$ of its direction, and its energy E. These variables are sufficient to define the state α of the particle where:

$$\alpha = \alpha(x, y, z;\ E;\ \theta, \phi) \tag{2.1}$$

The spherical coordinate system for defining the particle's direction is illustrated in figure (2.2).

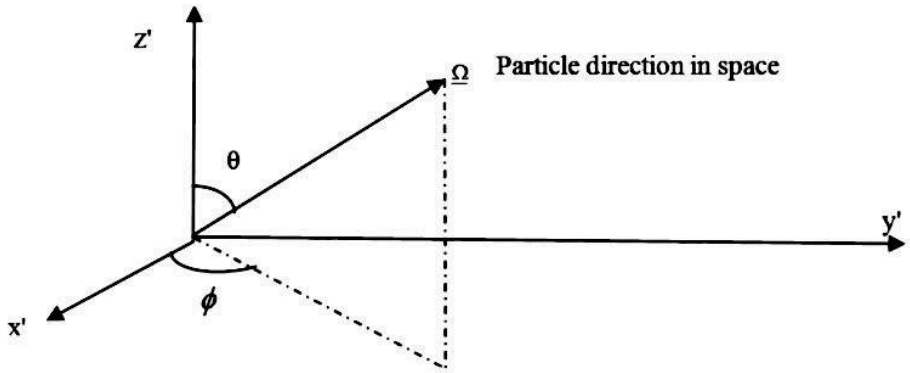

Fig (2.2) Particle's direction in spherical coordinates (θ, ϕ), the orthogonal coordinate system (x',y',z') is parallel to the basic reference system (x,y,z) shown in figure (2.1)

A particle trajectory from collision to collision can be constructed as a succession of states α_0, α_1, α_2, α_n, where i_{th} state is defined as

$$\alpha_i = \alpha_i(x_i, y_i, z_i; E_i;\ \theta_i, \phi_i) \tag{2.2}$$

That is, in the i_{th} state the particle has the spatial coordinates of the i_{th} collision point and the energy and direction of the particle after the i_{th} collision. With the exception of the initial state each successive state is a function only of the previous state, and scattering laws obeyed by the particle in the material of interest. Thus one could commence with initial or source conditions which define α_0 choosing by random sampling from the relevant probability distributions, the new values of the variable which determine α_1, and so on. In this way, individual life history can be constructed. In most Monte Carlo calculations, it is not necessary to store simultaneously every detail of the life history of every studied particle; usually, all that is required is the latest state of the particle being currently followed. This has obvious implication on computer storage requirements.

Obviously, specific mathematical procedures are required for selecting the position of the next collision point, the new energy and direction of the particle if it survives from that collision. Consider a particle which has just undergone its i_{th} collision (or scattering) and try finding the spatial coordinates of its next collision point.

If we denote s as the path length of the particle to the next collision point, the probability of a particle traveling a distance without having an interaction is $e^{-\Sigma s}\, ds$ where Σ is the particle's total cross section (denoted by μ in the case of photon).

A procedure for picking at random a value of s should be established from the probability function implied by the $e^{-\Sigma s}\, ds$.

For a moment, it should be assumed that such a procedure is available and that a particular value of s is selected to assign to s_i. Once the value of s_i is determined, the coordinates of the next collision point are readily found from,

$$X_{i+1} = x_i + s_i\,(sin\theta_i\, cos\emptyset_i)$$
$$Y_{i+1} = y_i + s_i\,(sin\theta_i\, sin\emptyset_i) \qquad (2.3)$$
$$Z_{i+1} = z_i + s_i\,(cos\theta_i)$$

The type of interaction must be decided again by sampling from the appropriate probability function. For the sake of illustration, it is assumed that it is again a scattering event. The energy and direction of particle after scattering is obtained by sampling from the appropriate scattering function. For example, in the case of a photon, the scattering process is Compton scattering and the probability function is given by the Klien-Nishina theory. By sampling, the new energy E_i, can be determined. Also, the local angles of the scattering event (θ_0, ϕ) illustrated in figure (2.3) can be determined.

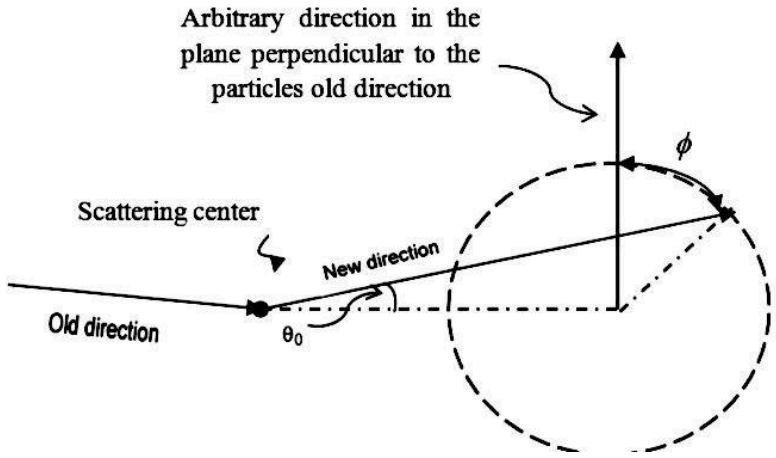

Fig (2.3) Particle's local angles of scattering. θ_0 is the deflection angle, and Φ the azimuthally angle [Wood 81]

The final problem is how to relate the particle's old direction $(\theta_{i-1}, \phi_{i-1})$ and the local angles (θ_0, ϕ) to determine the new direction of the particle (θ_i, ϕ_i).

A convenient (but not the only) method of doing this is to consider the spherical triangle defined on the unit sphere by the intersection of the surface of the sphere with the old and new directions of the particle and the direction of the reference polar axis of the system. The scattering point is considered the center of the unit sphere as in the following figure.

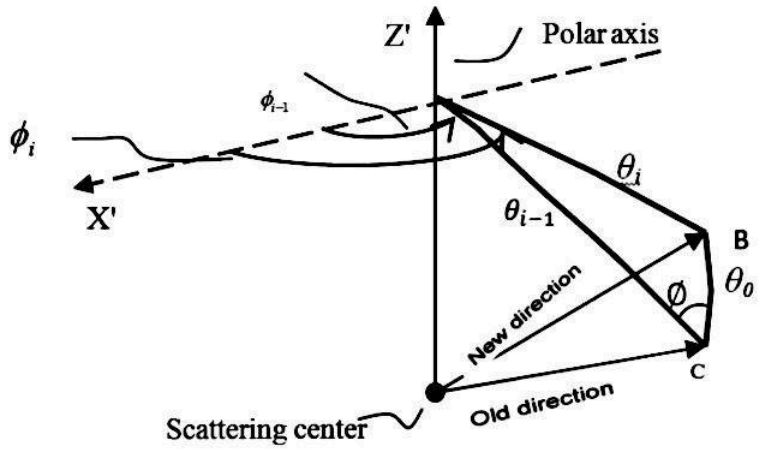

Fig (2.4) Geometry of spherical triangle ABC defined on the unit sphere. The spherical triangle has sides θ_{i-1} ,θ_i ,θ_0, and interior angles φ and (φ_i ,φ_{i-1})

By considering this spherical triangle and by utilizing standards relationships of spherical trigonometry, sines and cosines of θ_i and ϕ_i can be determined for use in equation (2.3), as follows:

From the law of cosines for spherical triangle, there is [Wood 81]:

$$\cos\theta_i = \cos\theta_{i-1}\cos\theta_0 + \sin\theta_{i-1}\sin\theta_0\cos\phi \qquad (2.4)$$

from which $\cos\theta_i$ can be determined. Next $\sin\theta_i$ can be determined from the well known identity:

$$\sin^2\theta_i + \cos^2\theta_i = 1 \qquad (2.5)$$

Now, invoking the law of sines gives:

$$\sin(\theta_i - \theta_{i-1}) = \frac{\sin\theta_0 \sin\phi}{\sin\theta_i} \tag{2.6}$$

Reapplying the law of cosines to get:

$$\cos\theta_0 = \cos\theta_{i-1}\cos\theta_i + \sin\theta_{i-1}\sin\theta_i\cos(\phi_i - \phi_{i-1}) \tag{2.7}$$

From which $\cos(\phi_i - \phi_{i-1})$ can be calculated.

Finally, the value of $\sin\phi_i$ and $\cos\phi_i$ can be deduced from the standard trigonometric formulas:

$$\sin\phi_i = \sin(\phi_i - \phi_{i-1})\cos\phi_{i-1} + \cos(\phi_i - \phi_{i-1})\sin\phi_{i-1} \tag{2.8}$$

$$\cos\phi_i = \cos(\phi_i - \phi_{i-1})\cos\phi_{i-1} - \sin(\phi_i - \phi_{i-1})\sin\theta_{i-1} \tag{2.9}$$

This completes the description of a set of a systematic procedure for constructing theoretical trajectories of the particles as they diffuse through the medium. Each particle is traced until its life history is terminated. When one particle is terminated (and score), a new particle life history started from the source and it is traced. What remains to be clarified, in this connection, are procedures for sampling from known probability functions.

2.4 Generating Random Numbers

It is central to the application of the Monte Carlo method that an adequate supply of numbers 'chosen at random' should be available. As previously mentioned, random numbers is a statistical term referring to a set of numbers; each of which is unrelated by any test that can be applied to its set members. In particular, many computer languages provide functions to generate such a series of numbers, the most prevalent form of which produces a sequence of numbers lying in the range 0-1 with equal probability. Technically, because the computer must generate random numbers by a known method, the numbers produced are often called "pseudo-random numbers" [Fish 86].

2.5 Variance Reduction Techniques

There are two basic ways by which the error in a Monte Carlo calculation can be reduced. The simplest way is to increase IMAX which represents the number of started particles. The other and the more sophisticated way is to reduce the standard deviation of individual samples. A number of different schemes have been proposed for reducing standard deviation. These are collectively referred to as variance reduction techniques. From a practical view point, an important characteristic of valid variance reduction technique is that it should lead to real saving of computing time. In the present study, the concept of survival weight is used as a variance reduction technique.

2.5.1 The method of survival weights

This device is one of the sophisticated concepts used in the program. The use of this device is best described by reference to theoretically computing the transmission ratio and spectrum of the photons that escape through a slab of shielding material placed in front of a source of radiation. In the Monte Carlo analog of the problem, if the slab is thick, relatively few of the particles that are started from the source would escape from the slap; the mostly they would absorbed in the slab and contributing little information on the energy of escaping particles. It is intuitively obvious that it would be more efficient to flow only those particles that experience only scattering collisions since they have the best chance of ultimately penetrating the slab.

However, if the particle is only permitted to scatter in the Monte Carlo schematization, the results of the calculation would be distorted. To counteract this, the particle's survival weight is adjusted after every

collision (which is perforce a scattering collision). For example when the particle leaves the source a survival weight of unity assigned for it. After its first collision, its survival weight is multiplied by the factor ($\mu_c(E)/\mu(E)$) which is simply the probability that the interaction is a scattering event. Following every subsequent collision, the particle's existing weight is similarly adjusted. This is accomplished by providing the particle with an additional "state" variable called weight.

With the introduction of this scheme into a Monte Carlo calculation, the particles survive every collision and it is necessary in practice to establish additional criteria (other than escaping the system) for terminating the life history. One possible criterion is to kill the particle when its energy becomes less than some pre-assigned cut-off energy [Wood 81].

The purpose of this computer program is to solve the problem of gamma ray reflection and transmission, for a gamma ray source uniformly incident on the left hand face of an infinite plane homogeneous slab of shielding material. The method used is the Monte Carlo technique, in which the life histories of a large number of particles (photons) are followed. In the particular form of the Monte Carlo method used here, there is a close analogy between the physicals and the mathematical particles followed by the program. The only sophistication employed is the concept of the survival weights. Thus we do not allow absorption of the photons as such; all collisions are forced to be Compton scatterings. The effect of absorption is accounted for by modifying the weight of the particle after each collision. That is the particle weight after a collision is the weight before collision multiplied by the survival ratio, $\mu_c(E) / \mu(E)$, which is of course the probability that a collision will be a Compton scattering. It is important to realise that is this, the basic form of the

program, the pair production event is regarded as a purely absorptive interaction.

In this version of the program, the history of each particle is followed until the particle either escape from the system or due to successive scatters, its energy drops below some preset minimum, in either event a new photon is started with an initial weight of unity.

2.6 Program Design

In this study, a Visual Basic computer program is designed and written to calculate gamma ray buildup factor for single layer shield of different materials. The program was utilized for simulating the classical problem of gamma rays beam incident on finite plane slabs of different absorbing materials. The geometry of source used in this program is plane normal source as illustrated in figure (2.5). This problem is a mathematical problem based on statistical probability theory. It is utilized in gamma transport problem. The penetration of radiation proceeds by compiling life histories of individual gamma ray as they move about, from the point where they are either absorbed in the shield or pass through it. The basic idea in the program is to compose a series of life histories of the source particles by using random sampling techniques to sample the probability laws that describe the real particle behavior, and to trace out the steps of the particles “random movement” through the medium.

The history of the particle is followed until it can no longer contribute information of interest to the problem in hand. The life history is then terminated and a new particle is started from the source. The applicability of the Monte Carlo technique arises from the fact that the macroscopic cross section may be regarded as the probability of the specific interaction per unit distance traveled by gamma photon.

A set of photons histories is generated by tracing individually the photon through successive collisions which results in scattering or absorbing.

The developed computer program, in this study, treats gamma ray penetration through the matter by taking into account the interaction of Compton scattering and pair production in a single layer shield.

To start the history of the first photon, it is necessary to determine where the photon has its photon collision. This is done by sampling the first collision probability distribution function $\rho(x) = \Sigma_t\, e^{\Sigma_t x}$ where Σ_t (total macroscopic cross section) is evaluated at energy E_o. The method for sampling such distribution function in random matter will be discussed later. Suppose that the selected value of (x) is x_i, and the thicknesses of (n) shield layers of different material are ($t_1, t_2, t_3, \ldots\ldots t_n$), then if (a) represent the total shield thickness, it is necessary to test x_i such that:

1- If x_1 > a, then the photon has penetrated the shield without collision, this journey is registered, and the history is terminated.

2- If x_1 < a, a collision occurred within the shield at the point x_1. Now to determine in which layer x_i lies, another comparison is made with different layer thickness, if $x_1 \leq t_1$then the photon is travelling in the first layer but if $x_1 > t_1$ it doesn't , and the same thing for remaining layers till the position of collision point is determined.

The method used is the Monte Carlo technique in which life histories of a large number of particles (photons) followed. In the particular form of the Monte Carlo method used here, there is a close analogy between the physical particles and the mathematical particles followed by the program. The only sophistication employed is the

concept of survival weights. Thus, absorption of the photons is not allowed as such, all collisions are forced to be Compton scattering or pair production. The effect of absorption is accounted for by modifying the weight of the particle after each collision. That is, a particle weight after a collision is obtaining by multiplying the weight before collision by survival ratio, μ_c / μ(E) (if we only take the effect of Compton scattering) which is of course the probability that a collision will be a Compton scattering. The applied strategy to account the effect of pair production interaction in this study can be summarized as follows, assuming that the pair production event can occur (i.e. E $\geq$ 1.022 MeV), then pair production is considered to occur if $\xi > \mu_c / (\mu_c + \mu_{pp})$, where ξ is a random number lying between 0 and 1, otherwise, a Compton scattering take place. In either event, the survival weight factor is given by SURV $= (\mu_c + \mu_{pp})/\mu(\mathrm{E})$. If pair production occurs, the original gamma photon is completely removed and replaced by 2 annihilation gamma photon of 0.511 MeV.

In this study, the history of each particle is traced until the particle either escapes from the system, or its energy drops below some preset minimum due to successive scatters. In either event, a new photon is started with an initial weight of unity. The position and direction of a photon are defined by 4 variables $(i.e.; Y, Z, \theta, \varphi)$, which are referred to as the coordinate system shown in figure (2.2)

The principal quantity computed and output by our developed program is the "dose buildup factor", which is a measure of how the transmitted photons are enhanced by Compton and pair production interactions.

An instructive feature of the program is that a record of the number of particles which suffer each of the possible fates is kept to facilitate

checking that all particles started from the source are correctly accounted for. The program has been deliberately written in a modular form, each subroutine or sub program is dedicated to do calculation for a distinctive physical event may occur along the photon journey in the shield.

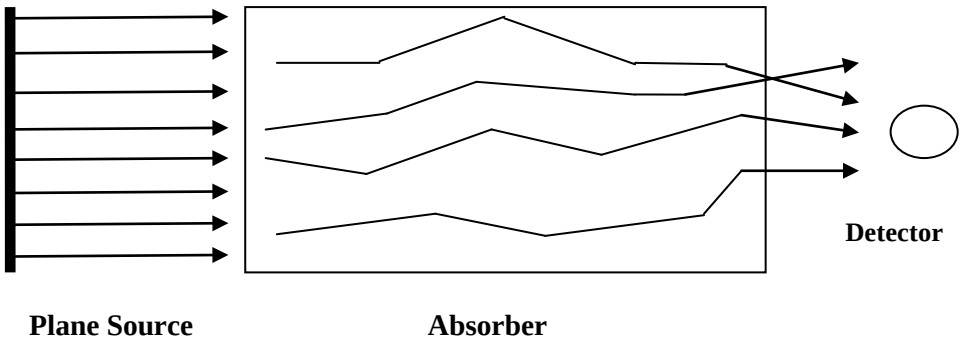

Fig (2.5) The geometry of plane normal source and shielding slabs considered by developed program

2.7 The Essential Subroutines Used in the Program

The flow diagram of the developed computer program is shown in figure (2.6), the purpose of each subroutine used in this program will be illustrated in the following paragraphs.

Glossary of Main Variable Names Considered in the Flow Diagram of Modified Program

I	Index labeling i^{th} particle history.
IMAX	Maximum number of particle histories to be studied.
E	Photon energy in MeV.
EMAX	Maximum photon energy in problem, i.e. the source energy. (EMAX ≤ 10).
JMAT	Counter stores the number of occurred "pair production" process.
NRU	It is a flag value used to refer the occurrence of RUSH step intermediate.
P	Photon's survival weight.
WRU	The weight of Russian Roulette.
PMIN	The minimum value of photon's survival weight.
EMIN	Cut-off energy in MeV.

NPAIR	A flag referring to occurrence of pair production.
SURV	The survival ratio: the probability for a photon of given energy which suffers a collision that the interaction will be a Compton scattering.
NCROS	A flag refer to the instance of "crossing the bar"... intermediate flag.

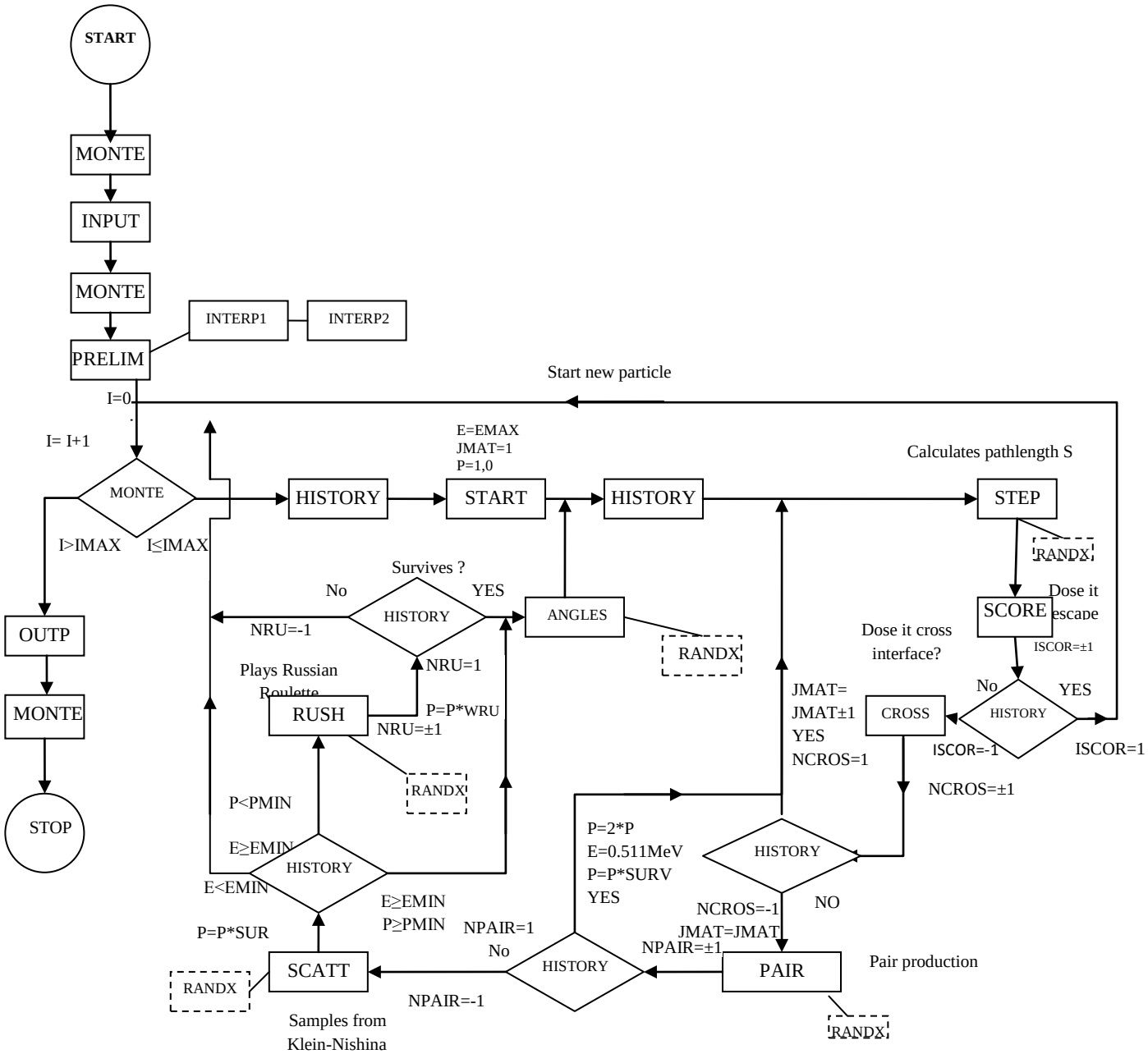

Fig (2.6) The flow diagram of modified program

2.7.1 MONTE

This is the segment of the program in which the calculation commences and ends. The principal function of MONTE is to ensure that the main sequence of the schematization is correctly followed. In addition to this, MONTE monitors the number of newly started particles.

2.7.2 INPUT

This subroutine is concerned with reading, in a formatted form, the basic shared data required by the program. This includes the simulation parameters and the energy dependent parameters (Compton cross section). This subroutine is repeated according to the number of layers considered in the simulated experiment.

2.7.3 PRELIM

Because of the large number of particles followed in a typical Monte Carlo calculation, it is desirable to minimize the amount of computation associated with each stage of a photon history. The efficiency of the corresponding program is greatly increased by: firstly, performing certain calculations, secondly, storing the results in a convenient form for subsequent usage. The task of this subroutine is to carry out these preparatory calculations our developed program.

It is unrealistic to presume that the cross section data can be put in such a way that, whatever the photon energy after a Compton scattering, there will be a corresponding value of the linear attenuation coefficient which is obtained immediately from the basic data table [Wood 81]. The procedure that we have adopted to deal with this problem is to read the basic data for a widely-spaced energy mesh, and have a sub program to construct its own detailed data tables for a fine wavelength mesh by interpolation in the basic data. The data corresponding to every photon wavelength is then efficiently obtained through using "look-up table

mechanism". The major function of PRELIM is to set up detailed cross section data table. For this purpose, it requires an interpolation procedure which is implemented in the auxiliary subroutine INTRP. Other tables constructed in BRELIM they are:

i) The values of the sine and cosine of any angle given in degrees.
ii) The energy mesh tables for storing the spectra of the photon exiting from the system [Wood 81].

As mentioned earlier, this subroutine also repeats the calculation for each layer considered in the shield.

2.7.4 HISTORY

The particular path taken by each photon through the slab layer is controlled by this subroutine. The route followed depends on various decisions taken by HISTORY. These decisions depend principally on the wavelength of the photon and whether it escapes from the system. In particular, if the photon does not escape from the system, it must be made to scatter again. To escape completely from the system, a photon traveling to the right must penetrate the total thickness of the shield under consideration.

2.7.5 START

The initial vales of the variables required to variables which define a photon’s state are given their initial values in this subroutine, thus the particular type of source considered is imposed here. Now, the photon is considered to begin his journey from the first layer of the shield.

2.7.6 STEP

This subroutine performs three essential tasks:

i. It establishes after a collision, the position of the photon in the fine mesh wavelength table, for subsequent look–up of the cross section tables.
ii. It selects randomly, the path length of the photon to the next collision point, using for this purpose the method of inverse cumulative function which will be described later.
iii. By means of equation (2.3), it computes the coordinates of the next (postulated) collision point.

In connection with (i) it is essential that the method employed is compatible with the tables constructed in subroutine PRELIM. This is an important point to remember; it should it ever be thought necessary to alter the existing wavelength structure.

2.7.6.1 The Inverse Cumulative Function Method

This method is used to select randomly the path of the photon to the next collision point in subroutine STEP. One of the most important and mathematically attractive method for selecting variates relies on the fact that random variable from any given pdf (probability distribution function) can be expressed as a function of another random variable that is uniformly distributed between zero and one (i.e. from the canonical distribution) [Wood 81].

Consider x distributed as $P(x)$, and let $y = f(x)$ denotes a monatomic increasing function of x, and let $g(y)$ denote the distribution of the random variable y, now clearly, when $x \leq a$, then $y \leq f(a)$. This can be interpreted as,

$$Prob\ (x \square a) = Prob\ (y \leq f(a))$$

Restating this equality in terms of the respective cumulate distribution function, given

$$P(a) = \int_{-\infty}^{a} P(x)dx = \int_{-\infty}^{f(a)} g(y)dy \qquad (2.10)$$

Now, if we choose $g(y) = 1$, for $0 \leq y \leq 1$ (i.e. $g(y)$ is the canonical distribution), then,

$$P(X) = \int_{-\infty}^{X} P(x')\,dx' = \int_{-\infty}^{\xi} dy = \xi \qquad (2.11)$$

That is,

$$x = P^{-1}(\xi) \qquad (2.12)$$

That is, from any arbitrary probability density function (pdf), by the transform to the inverse cumulative distribution function (P^{-1}), a random number from the canonical distribution can be sampled. In practice, this method is only applicable if we can fairly easily perform the "inverse operation" that required by equation (2.12).

To show that the sample values of x obtained from equation (2.12) are indeed from the desired pdf, consider the graph in figure (2.7) which illustrates the procedure. From figure (2.7), it is clear that:

Probability that x lies in the interval $(x, x + \Delta x)$ = probability that y lies in $dy = g(y)\,dy = dy, (since\ g(y) = 1) = dp(x)$

Thus, the sample values of x have the required distribution. In the discussion of particle trajectory, the path length of a particle (photon) to the next collision point was obtained by sampling the pdf,

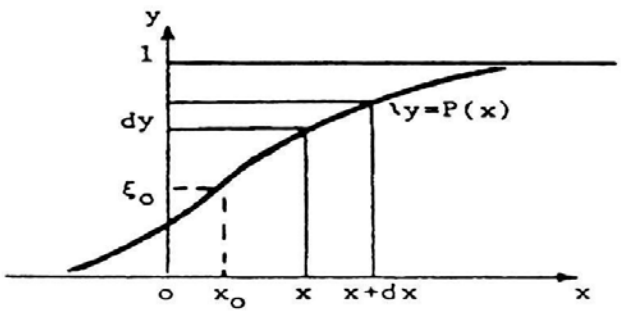

Fig (2.7) Graph of cdf p(x). The random number ξ_0 determines x_0 [Wood 81]

$$P(x) = \mu e^{-\mu x}, \quad 0 \leq x \leq \infty \tag{2.13}$$

Where μ is the linear attenuation coefficient of the medium. By substituting equation (2.12) in (2.13) it can be concluded that

$$X = \frac{1}{\mu}\log_e(1-\xi) \tag{2.14}$$

But (1-ξ) is distributed as ξ, therefore

$$X = -\frac{1}{\mu}\log_e \xi \tag{2.15}$$

Hence, the x-values obtained from equation (2.15) are equivalent to randomly sampling from the pdf which cover the photon's path length in homogenous medium, and this is the procedure used in subroutine STEP.

2.7.7 SCATT

In this subroutine, the new wavelength after a Compton scattering is selected by sampling from the K-N (Klein – Nishina) distribution. The particular sampling technique used is that of Khan (which will be described later); once the new wavelength is found, the Compton angle of scattering θ is readily determined. Another function of SCATT is to modify the particle weight P to its new value after a scattering. It should be mentioned that, in the Compton scattering interaction, a primary photon is absorbed via its interaction with an orbital electron. The latter is freed and a secondary or scattered photon of energy lower than the primary is created. The basic theory of this effect, which assumes the electron to be free and at rest is that of Klien and Nishina (1929). This basic theory has been well confirmed experimentally. It is true that some departures from it may occur for low and high energies of the incident photon. From the point of view of shielding applications in most of the

energy range where Compton scattering is a major contribution in the total cross section, the Klien – Nishina (K-N) theory is directly applicable.

In figure (2.8), θ is the Compton angle scattering, and ϕ is the azimuthally angle of scattering. The shielding studies indicated that ϕ is uniformly distributed between 0^0 and 360^0 [Evan 55].

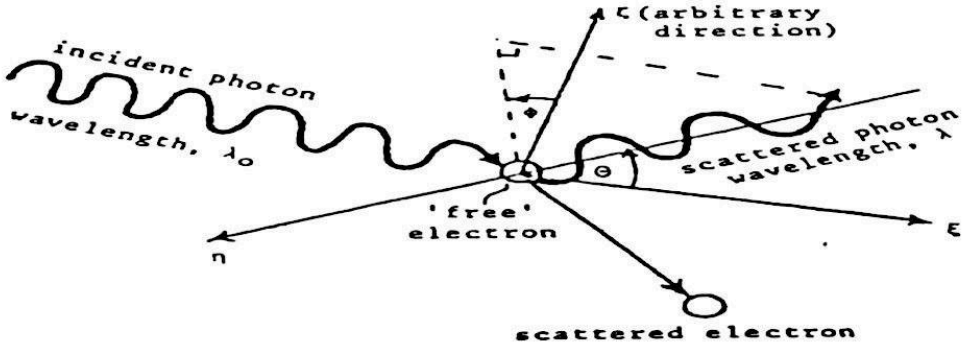

Fig (2.8) Geometrical relation in a Compton scattering events. The local orthogonal axis (ξ,η,ζ) are constructed such that ξ lies along the original direction of the photon's travel [Wood 81]

Compton cross section (σ_c) is often expressed in units of barn per electron (b/electron). A simple conversion factor can then be used to compute the contribution of Compton Effect (μ_c) to the total cross section for a particular material. K-N theory also provides a result that is essentially needed in Monte Carlo simulation of photon transport, namely the scattering probability density function $f(E)$. As had been noticed, a key feature of Monte Carlo method is the use of random numbers to sample from the probability density functions that are considered to describe the physical behavior of the particles.

The pdf $f(E)$ for the photon energy E after Compton scattering is directly deducible from K-N theory. In practice, instead of using energy variable E, it is usually more convenient with an energy related variable x (which is defined latter), and to sample at random from the K-N pdf $f(x)$.

Even then the form of $f(x)$ is relatively complicated and simple sampling techniques do not prevail.

2.7.7.1 The Klein Nishina Formula

The relationship between photon deflection and energy loss for Compton scattering on the assumption that the electron to be free and stationary, is determined from consideration of conservation of momentum and energy between the photon and recoiling electron.

$$\frac{E}{E_0} = \frac{1}{1 + (\frac{E_0}{m_e c^2})(1 - \cos\theta)} \tag{2.16}$$

where E_0 and E are, respectively; the energies of the photon before and after the collision in MeV. The electron rest energy is m_0c^2 and θ is the photon deflection angle (see figure 2.8).

In gamma rays transport calculations, it is usually more convenient to use, instead of energy variable, the wavelength of the photon in Compton units, namely $\lambda = 0.511/E$ where E is the photon energy in MeV. The increase of the photon wave length associated with the Compton scattering events is

$$\lambda - \lambda_0 = 1 - \cos\theta \tag{2.17}$$

where λ_0 and λ are in Compton units, and λ_0 is the wavelength of the photon before scattering and λ is the wave length after scattering. Clearly the maximum shift in wave length is two Compton units. It occurs when the photon has been deflected through 180^0. In Monte Carlo simulation of photon transport, it is necessary to know, after a Compton scattering, the angle of scattering θ, and the new value of the wavelength λ. The most commonly used procedure for obtaining these quantities is by

sampling using the K-N pdf f(x) to find the value of (x) after a scattering, and deduce θ from equation (2.17),where x is defined as $x = \lambda/\lambda_o$.

When the angular dependence of the scattered photon integrated, in terms of the dimensionless variable x, the Klein – Nishina differential cross section will take the following compact form;

$$d\sigma = k\left(A + \frac{B}{x} + \frac{C}{x^2} + \frac{D}{x^3}\right)dx \quad 1 \le x \le 1 + 2\alpha_o \tag{2.18}$$

$$\alpha_o = \frac{1}{\lambda_o} = \frac{E_o}{0.511} \tag{2.19}$$

$$x = \frac{\lambda}{\lambda_o} = \frac{E_o}{E}$$

And E_0 is the incident photon energy in MeV.

Additionally,

$$k = \pi\frac{r_e^2}{\alpha_0}, \quad (r_e^2 = (\frac{\mu_0 e^2}{4\pi m_e})^2 = 7.94077 * 10^{-26} cm^2) \tag{2.20}$$

also,

$$A = \frac{1}{\alpha_0^2}, \quad B = 1 - 2\frac{(\alpha_0 + 1)}{\alpha_0^2}, \quad C = \frac{(1 + 2\alpha_0)}{\alpha_0^2}, \text{ and } D = 1$$

The total Compton cross section is obtained by making integration on equation (2.18), hence

$$\sigma_C = \int_1^{1+2\alpha_0} d\sigma = k'\left[\frac{4}{\alpha_0} + (1 - \frac{1+\beta}{\alpha_0^2})\frac{\gamma}{2}\right] b/electron \tag{2.21}$$

$$k' = k \times 10^{24}$$

$$\beta = 1 + 2\alpha_0$$

$$\gamma = 1 - \beta^{-2}$$

It is clear from equation (2.21) that σ_C is a function only of the incident energy of the photon. The pdf f(x) for the Compton scattering process correspond to $\frac{d\sigma/dx}{\sigma_C}$; therefore it has the form

$$f(x)=\begin{cases} H(A+\frac{B}{x}+\frac{C}{x^2}+\frac{D}{x^3}), & if \quad 1\le x\le 1+2\alpha_0 \\ 0, elsewhere, \end{cases} \tag{2.22}$$

where $H = k'/\sigma_C$.

The pdf in the variable E and x are simply related, as follows

$$f(E)dE = f(x)dx \tag{2.23}$$

From the previous definitions of σ_C and $f(x)$, it is immediately apparent that f(x) satisfies the basic requirement for every pdf, namely,

$$\int_{-\infty}^{\infty} f(x)dx = 1 \tag{2.24}$$

For completeness, to determine the new direction of the photon in space, it is necessary to know in addition to θ, the azimuth angle ϕ (see figure (2.8)). This is readily obtained by sampling, randomly, for any angle lying between 0^0 and 360^0 with equal likelihood which presents no practical difficulty [Wood 81].

2.7.7.2 The Khan Method

Khan method is the most widely used technique for sampling from K-N pdf. It does not rely on any approximation and is valid for every energy of the incident photon. But it permits repeated rejection before an acceptable value of x is found. Consequently, it is relatively expensive in its use of random numbers and computing time. This method is based upon the composition rejection technique; the summarization of this technique can be described as follows:

Suppose that a given probability is capable to being expressed in the form of a finite sum of terms, thus

$$P(x) = constant \times \sum_{i=1}^{N} \alpha_i g_i(x) h_i(x), \tag{2.25}$$

where, $\sum_{i=1}^{N} \alpha_i = 1$

And, for the range of x upon which P(x) is defined, g_i and h_i have the following properties:

$g_i(x)\ is\ a\ pdf, and\ hence\ \int g_i(x)dx = 1$

$0 \leq h_i \leq 1, for\ i = 1,2, \ldots . N$

Then sampling can be made from P(x) in the following manner: select a value of i with probability α_i and sample from $g_i(x)h_i(x)$ by the generalized rejection method (that is, sample from $pdf\ g_i(x)$ by the inverse cumulative function method and from $h_i(x)$ by the rejection method).

2.7.8 ANGLES

This subroutine performs the vital role of determining the variable $(\theta_{n+1}, \emptyset_{n+1})$ which define new direction of the photon after a Compton scattering. The trigonometric relationships for the spherical triangle, depicted in figure (2.9), the trigonometric relationships can be solved to obtain the new values, because the program has knowledge of:

(a) The previous values of the angles $\theta, \emptyset$.

(b) The latest scattering angle.

(c) The azimuthally angle of scattering $(\emptyset)$ which is assumed to be distributed uniformly in the range between $(0^0 - 360^0)$.

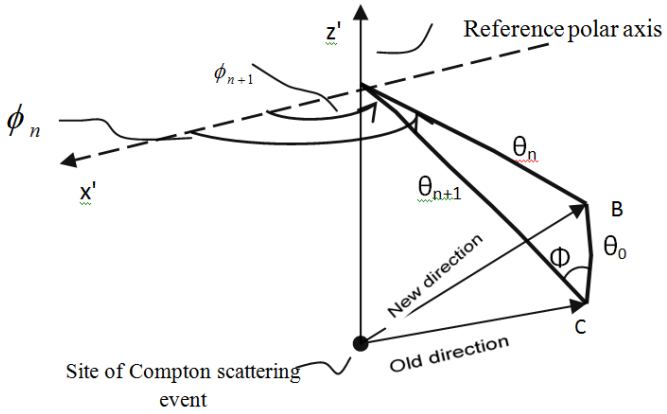

Fig (2.9) The spherical triangle formed by the photon's previous direction and its new direction after a Compton scattering [Wood 81]

2.7.9 SCORE

If a photon penetrated a slab thickness, its contribution to the score at the appropriate boundary must be recorded; this is the essential purpose of SCORE. Therefore, this subroutine must obtain answers to the following questions with respect to the next collision point.

(a) Does the photon cross an interface? if so this means a photon enters a new material. The score at that interface must be suitably adjusted, and the problem should alter for dealing with the parameters of the new material.

(b) Can the photon still scatter again in the system? Bearing in mind that a number of slab thicknesses are being simultaneously considered, or does the photon escape entirely?

To assist SCORE in these considerations, it is important to ascertain immediately on entry to the subroutine, the direction in which the photon is traveling (i.e. to the right or to the left).

The scoring photons are classified twice:

(1) According to their z-value when they cross a boundary.

(2) According to their position in the energy spectrum table.

This information is passed to subroutine OUTP for processing in the final stages of the calculation. The flow diagram of subroutine SCORE is shown in figure (2.10).

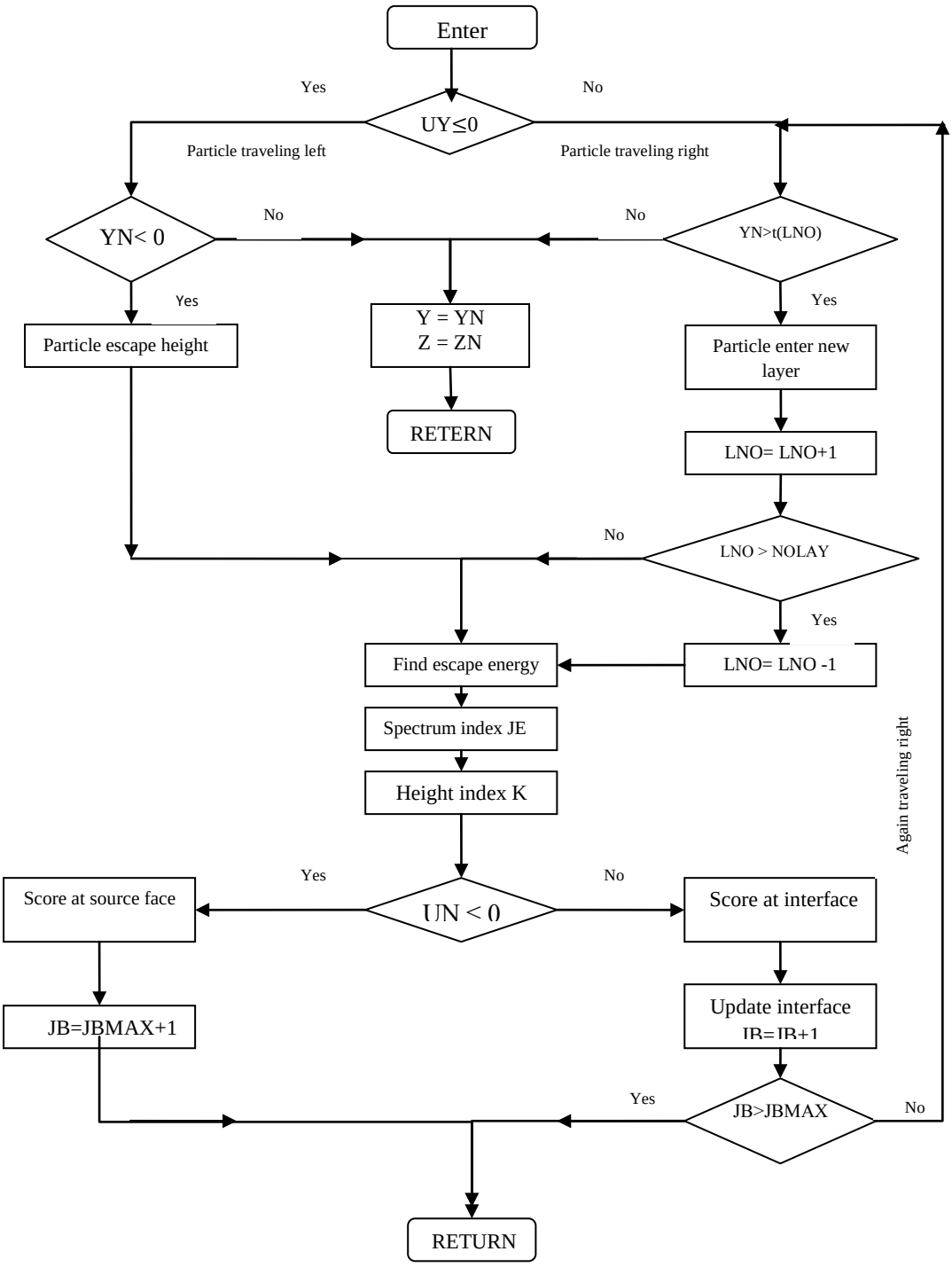

Fig (2.10) The flow diagram of subroutine SCORE in our developed program

Glossary of Main Variable Names Used in Subroutine Score

UY	Direction cosine, sinθ sinϕ.
YN	Postulated Y-coordinate of photon at next collision.
t (LNO)	Thickness of slab layer currently considered.
y	Y-coordinate of photon.
Z	Z-coordinate of photon.
ZN	Postulated Z-coordinate of photon at next collision.
LNO	Index denoting particular layer number that is currently being considered.
NOLAY	Total number of slab layers being considered in the problem.
JB	Index labeling the next right hand interface at which the photon can score if it crosses going right.
JBMAX	Maximum number of shield interfaces considered in the problem.

2.7.10 PAIR

The developed strategy of PAIR work flow is summarized in this section. Assuming that the pair production event can occur (E greater or equal to 1.022MeV), then pair production is considered to occur if $\xi > \mu_c/(\mu_c + \mu_{pp})$, where ξ is a random number, lying between $(0\ and\ 1)$; otherwise, a Compton scattering takes place. In either event, the survival weight factor is given by $SURV = (\mu_c + \mu_{pp})/\mu$.

where μ_c and μ_{pp} are given by:

$$\mu_c = (\frac{A_v}{A})\, Z\, \sigma_c \tag{2.26}$$

$$\mu_{pp} = \left(\frac{A_v}{A}\right)\, \sigma_{pp} \tag{2.27}$$

where:

μ_c = Attenuation coefficient of Compton scattering.

A_v= Avogadro's number.

A= Atomic weight.

Z= Atomic number.

σ_c= Compton cross section.

σ_{pp}= Pair production cross section.

μ_{pp}= Attenuation coefficient of Pair production.

The Compton cross section [Gold 59] and Pair production cross section [Evan 55] are given by:

$$\sigma_c = \frac{3}{4}\{\frac{1+E}{E^3}\ [\frac{2E(1+E)}{1+2E} ln(1+2E)] + \frac{1}{2E} ln(1+2E) - \frac{1+3E}{(1+2E)^2}\} \quad (2.28)$$

$$\sigma_{pp} = \sigma_o Z^2 (\frac{28}{9}\ ln\ (\frac{2E}{m_\circ c^2}) - \frac{218}{27}) \quad (2.29)$$

2.7.11 RUSH

This subroutine is concerned with a low weight or weak particle and decides its fate, weather continues its life history or not. Suppose that after a scattering collision a particle's survival weight is tested and found to be less than the low weight particle (given as P_{min}), say, a 1 in 10 chance of survival, This is implemented in the computer as follows: a random number ξ_1 within the range 0 to 1, is selected. If it is equal to or less than 0.1, the particle survives and, to avoid biasing, its weight is multiplied by 10. If ξ_1 is greater than 0.1, the particle is killed and its life history is terminated this method called Russian Roulette.

Russian roulette is the colorful name given to a game. It could be argued that Russian roulette is not strictly speaking a variance reduction technique as it introduces an additional degree of randomness into the calculation. While this may be true in theory, the method is in practice, an extremely useful mechanism whereby unimportant calculations may be considerably reduced and computing time significantly saved [Wood 81].

2.7.12 INTRP

This subroutine is called by BRELIM to provide the interpolated value of the basic data required in constructing the detailed data tables,

and it is essentially independent of the reminder of the program. The particular interpolation scheme used is Cubic Spline, a spline is a polynomial established to compute the interpolated points lay between each pair of tabulated points, but whose coefficients are determined "slightly" non-locally. The non-locality is designed to guarantee global smoothness in the interpolated function up to some order of derivative.

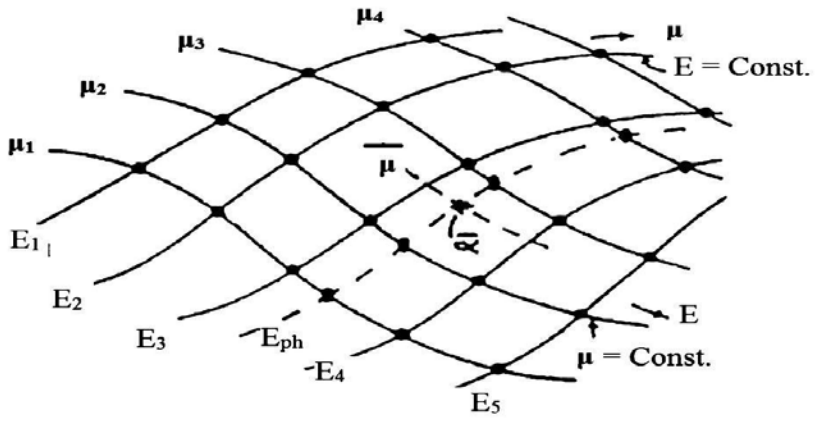

Fig (2.11) The surface formed by the data points. The points ( ) are formed by interpolating along each curve where (μ=constant)

Cubic splines are the most popular interpolation methods. They produce an interpolated function that is continuous through to the second derivative. Splines tend to be more stable than fitting other type of a polynomial representation, with less possibility of wild oscillations between the tabulated points.

We start from a table of points (x_i, y_i) for $i = 0, 1, \dots, n$, calculated from the function $y = f(x)$. This makes $n + 1$ points with n intervals between them. The cubic spline interpolation is a piecewise continuous curve, passing through each of the values in the table. There is a separate cubic polynomial for each interval, each with its own coefficients:

$$S_i(x) = a_i(x - x_i)^3 + b_i(x - x_i)^2 + c_i(x - x_i) + d_i \quad (2.30)$$

$$for\ x\ \epsilon\ [x_i, x_{i+1}]$$

Since there are n intervals and four coefficients (a_i, b_i, c_i, d_i) for each, so we need a total of 4n parameters to define the spline $S(x)$. We need to find 4n independent conditions to fix them. We get two conditions for each interval from the requirement that the cubic polynomial match the values of the table at both ends of the interval:

$$S_i(x_i) = Y_i \ , \quad S_i(x_{i+1}) = Y_{i+1} \qquad (2.31)$$

Notice that these conditions result in a piecewise continuous function.

We need 2n more conditions. Since we would like to make the interpolation as smooth as possible, we require that the first and second derivatives also be continuous:

$$S_{i-1}^{`}(x_i) = S_i^{`}(x_i) \ , S_{i-1}^{``}(x_i) = S_i^{``}(x_i) \qquad (2.32)$$

These conditions are applied for $i = 1, 2, \ldots, n-1$, resulting in $2(n-1)$ constraints.

2.7.13 RANDX

This is an auxiliary function which provides the random numbers that are essential to the Monte Carlo method. This subroutine depends on the Visual Basic function RND[(n)] which is in turn generate a single-precision random number between 0 and 1. In this function n is a numeric expression that specifies a value less than zero, zero, or more than zero. The RND function interprets each of these types of values as follows [MSDN]:

(i) If n < 0 supplies the same random number every time.
(ii) If n = 0 provides the last random numbers generated.
(iii) If n > 0 generates a new random number.

In our program, the value of (n) is chosen to be, always, greater than zero.

Chapter Three

Result and Discussion

3.1 Introduction

This chapter is dedicated to present the results of the established computer program that based on Monte Carlo method to calculate gamma ray buildup factor for a single-layer shield of aluminum, iron and lead. The choice of these materials is due to their importance in reactor shielding, the buildup factor was calculated with thickness in the range 1-5 mfp, and with energy range 4-10 MeV. The studied parameters can be categorized in terms of abroad scale into two types, the first type consists of the parameters concerted with the accuracy of the result obtained by applying Monte Carlo simulation computer program (i.e., number of scenarios, number of particles, and number of interval slice used to partition the photon energy spectrum); these parameters are called simulation parameters. The second type represents the physical parameters affecting the results of buildup factor (i.e., shield thickness, atomic number of the shield and the photon energy). Before presenting the results, we will demonstrate the input data to the simulation program which was built and applied in this study.

3.2 Input Data

The input data in our designed computer program can be classified into two groups:

3.2.1 Simulation parameters

The following simulation parameters were considered as:

1. Maximum number of particle's life histories to be studied. It was taken as 20000.

2. Total number of coarse mesh energies for which the corresponding basic cross section data has to be assigned into program. In this study the coarse mesh was set 28.
3. Number of photon intervals required in the photon energy spectrum table; it was set 12.

3.2.2 Physical parameters

The following physical parameters were considered:

1. The atomic number of the materials, different (light, medium and heavy weighted) materials have been chosen in this work: aluminum (Z= 13), iron (Z= 26), and lead (Z= 82); these materials are usually used for shielding.
2. Density of materials aluminum is 2.7 g/cm^3, iron is 7.8 g/cm^3 and lead is 11.34 g/cm^3.
3. Thickness in terms of mean free path of the shield material; the range of values 1 to 5 mfp is taken.
4. Cutoff energy; when photon energy becomes less than cutoff energy, its life history is terminated. In this work, the cutoff energy is taken to be 0.019MeV for Aluminum and 0.022MeV for Iron and 0.025 for Lead.
5. Conservation factor for the slab materials is set equal to N_A*10^{-24}/A; so, for aluminum = 0.022379, iron = 0.01056, lead = 0.0029065.
6. The photons applied energy is partitioned into 28 intervals, which covers the range 4-10 MeV. The partitions of the energy intervals (in MeV) are listed in the following list [Wood 81].

30	20	15	10	8	6	5
4	3	2	1.5	1	0.8	0.6
0.5	0.4	0.3	0.2	0.15	0.1	0.08
0.06	0.05	0.04	0.03	0.02	0.015	0.01

7. Table (3.1) lists the values of mass absorption coefficient data for air, in (cm^2/g), versus the photon energies values.

Table (3.1) Mass absorption coefficient data, for air in cm^2/g corresponding to the energies values [Wood 81]

Energy in MeV	μ_{air}	Energy in MeV	μ_{air}
30	0.0146	0.5	0.0297
20	0.0145	0.4	0.0295
15	0.0155	0.3	0.0287
10	0.0156	0.2	0.0268
8	0.0163	0.15	0.025
6	0.0173	0.1	0.0234
5	0.0182	0.08	0.0243
4	0.0195	0.06	0.0305
3	0.0211	0.05	0.0406
2	0.0237	0.04	0.0668
1.5	0.0256	0.03	0.148
1	0.028	0.02	0.512
0.8	0.0289	0.015	1.27
0.6	0.0296	0.01	4.63

8. Table (3.2) lists the mass attenuation coefficients data, in cm^2/g, for all materials studied in this work. Figures (3.1 A, B and C) show the behavior of total mass attenuation coefficients with Compton scattering, photoelectric absorption and pair production as functions of energy.

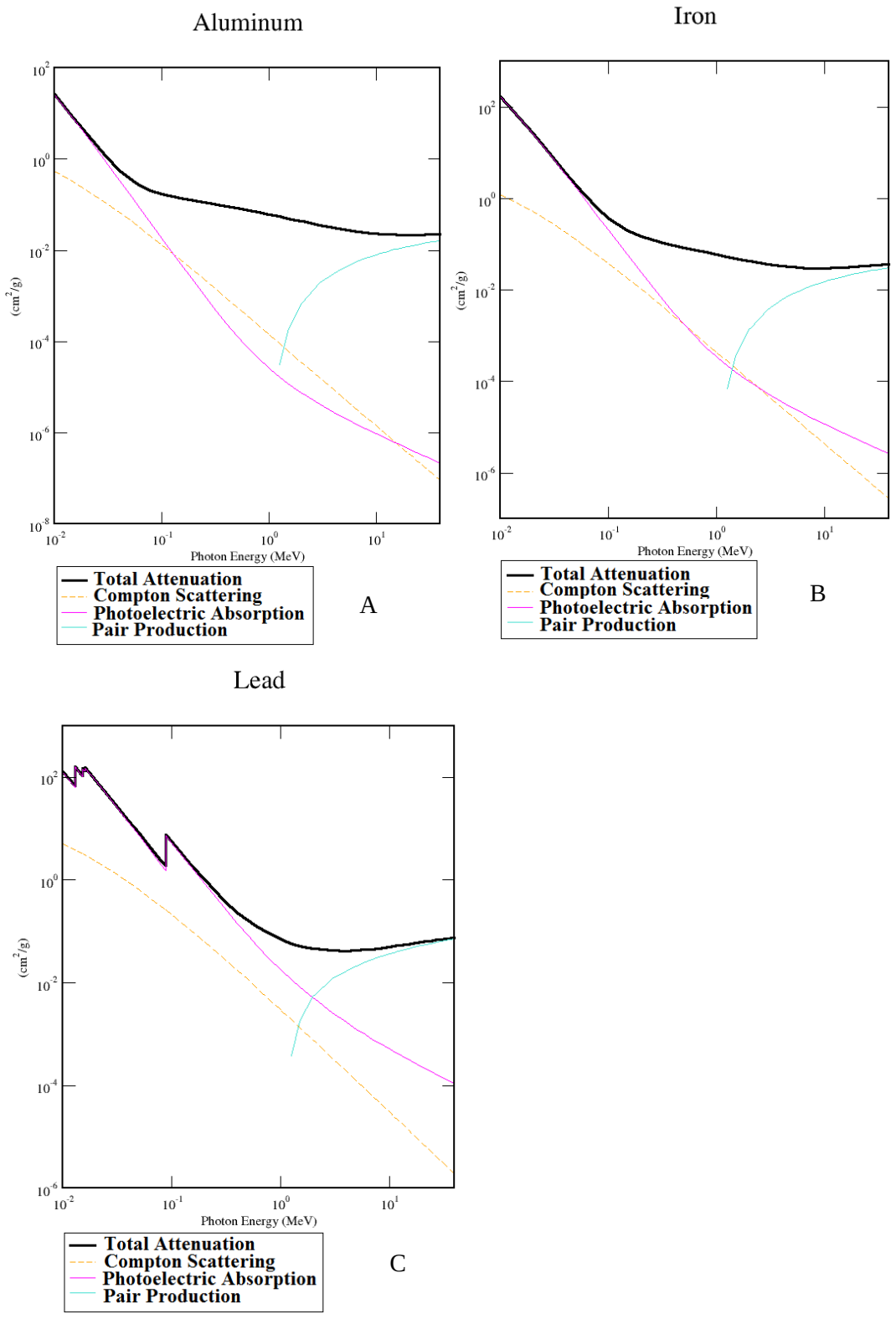

Fig (3.1) The behavior of mass attenuation coefficient versus photon energy, for (A) aluminum, (B) iron, (C) lead

9. Compton crosses section and Pair production crosses section; the corresponding cross section data at each energy interval mesh in (barn/atom) were extracted and tabulated in table (3.3).

Table (3.2) The mass attenuation coefficient μ (cm^2/g) for Compton scattering μ_c and pair production μ_{pp} for aluminum, iron and lead corresponding to energy interval in MeV mesh data [Xcom]

Energy in MeV	Al			Fe			Pb		
	μ_c	μ_{pp}	μ_{total}	μ_c	μ_{pp}	μ_{total}	μ_c	μ_{pp}	μ_{total}
0.5	0.0837	0	0.0837	0.0806	0	0.0806	0.0673	0	0.0673
0.6	0.0775	0	0.0775	0.0747	0	0.0747	0.0626	0	0.0626
0.8	0.0681	0	0.0681	0.0657	0	0.0657	0.0553	0	0.0553
1	0.0612	0	0.0612	0.0591	0	0.0591	0.0499	0	0.0499
1.022	0.0606	0	0.0606	0.0585	0	0.0585	0.0494	0	0.0494
1.25	0.0548	0.000031	0.05483	0.0529	0.000070	0.05297	0.0447	0.00037	0.0450
1.5	0.0498	0.000170	0.0499	0.0481	0.000358	0.04845	0.0407	0.00180	0.0425
2	0.0425	0.000674	0.04317	0.0410	0.001364	0.04236	0.0348	0.00545	0.04025
3	0.0334	0.001918	0.03531	0.0323	0.003781	0.03608	0.0274	0.01192	0.03932
4	0.0279	0.003102	0.03280	0.0269	0.006039	0.03293	0.0229	0.01712	0.04002
5	0.0241	0.004154	0.2825	0.0232	0.008032	0.03123	0.0197	0.02148	0.04118
6	0.0213	0.005098	0.02639	0.0205	0.009810	0.03031	0.0174	0.02523	0.04263
7	0.0191	0.005937	0.02503	0.0185	0.01139	0.02989	0.0157	0.02853	0.04423
8	0.0174	0.006694	0.02409	0.0168	0.012181	0.02898	0.0143	0.03151	0.04581
9	0.0160	0.007377	0.02337	0.0154	0.01409	0.02949	0.0131	0.03421	0.04731
10	0.0148	0.007999	0.02279	0.0143	0.01526	0.02956	0.0121	0.03671	0.04881

Table (3.3) The cross section (barn/atom) for Compton scattering σ_c and pair production σ_{pp} for aluminum, iron and lead corresponding to energy interval in MeV mesh data [Xcom]

Energy in MeV	Al			Fe			Pb		
	σ_c	σ_{pp}	σ_{total}	σ_c	σ_{pp}	σ_{total}	σ_c	σ_{pp}	σ_{total}
0.5	3.752	0	3.752	7.497	0	7.497	23.17	0	23.17
0.6	3.474	0	3.474	6.929	0	6.929	21.55	0	21.55
0.8	3.053	0	3.053	6.097	0	6.097	19.05	0	19.05
1	2.746	0	2.746	5.486	0	5.486	17.18	0	17.18
1.022	2.717	0	2.717	5.428	0	5.428	17.01	0	17.01
1.25	2.456	0.00140	2.457	4.908	0.00652	4.9145	15.40	0.1301	15.53
1.5	2.232	0.00765	2.232	4.462	0.0332	4.4952	14.02	0.6215	14.64
2	1.905	0.03023	1.935	3.809	0.1265	3.9355	11.98	1.875	13.85
3	1.499	0.08595	1.584	2.997	0.3506	3.3476	9.440	4.102	13.54
4	1.250	0.1390	1.389	2.501	0.5600	3.061	7.879	5.891	13.77
5	1.080	0.1861	1.266	2.160	0.7449	2.9049	6.806	7.389	14.19
6	0.954	0.2284	1.182	1.906	0.9097	2.8187	6.017	8.680	14.69
7	0.857	0.2660	1.123	1.716	1.056	2.772	5.409	9.816	15.22
8	0.780	0.2999	1.079	1.562	1.188	2.75	4.923	10.84	15.76
9	0.717	0.3305	1.047	1.435	1.307	2.742	4.526	11.77	16.29
10	0.665	0.3584	1.023	1.330	1.415	2.745	4.193	12.63	16.82

3.3 The Effect of Designed Shielding Parameters

Before we start to percent the effect of the designed shielding parameters, it should be mentioned that these parameters was studied in the absence (of Compton scattering effect) and presences of the effect of Compton scattering in addition to the effect of pair production.

3.3.1 The number of simulated photons

In any simulation problem the major question is how many repeated instance are needed to reach a chosen level of precision in the results. Table (3.4) presents the stability of buildup factor in terms of its standard deviations verses the iteration number for lead layer with thickness 1mfp initiated photon and energy 10 MeV.

Table (3.4) The standard deviation of buildup factor versus the number of iteration for Pb layer with 1mfp and E= 10MeV

No.	Iteration number	Standard deviation	No.	Iteration number	Standard deviation
1	100	0.1356	9	6000	0.0169
2	200	0.0962	10	8000	0.0146
3	400	0.0676	11	10000	0.0131
4	600	0.0548	12	15000	0.0107
5	800	0.0474	13	20000	0.00927
6	1000	0.0422	14	25000	0.00829
7	2000	0.0295	15	30000	0.00757
8	4000	0.0207	16	35000	0.00701

The relation between the standard deviation of simulated buildup factor verses the number of iteration are shown in figures (3.2) and (3.3) for the energy 1 MeV and 10 MeV, respectively, and thickness 1mfp.

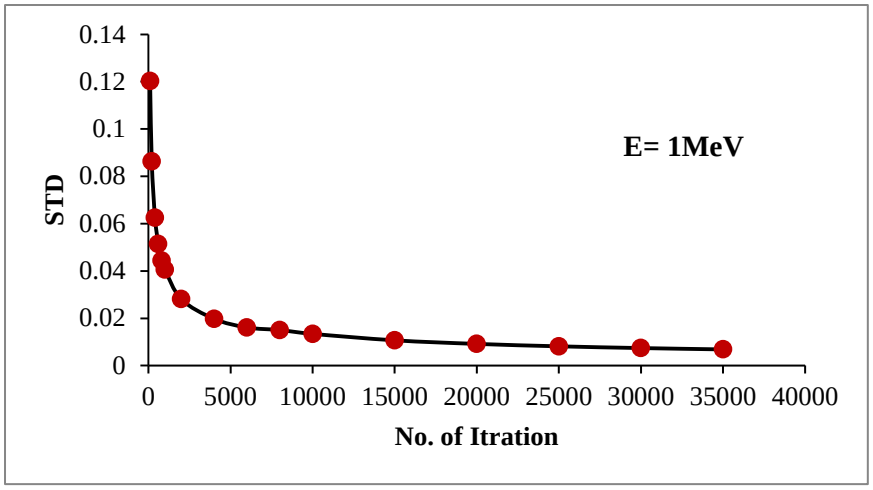

Fig (3.2) The effect of iteration number on the standard deviation of the simulated buildup factor for E= 1MeV

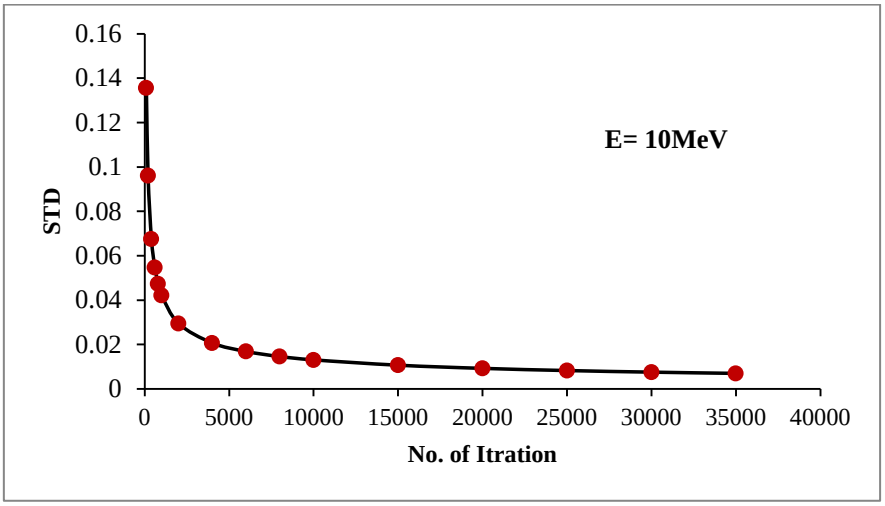

Fig (3.3) The effect of iteration number on the standard deviation of the simulated buildup factor for E= 10MeV

Figures (3.2) and (3.3), show that the increase in the number of iteration leads us to more convergence (i.e., stability) in the values of buildup factor.

In this simulation we have used the number 20000 of simulated photons to obtain simulated value of gamma ray buildup factor with more convergence. It is clear that the precision of simulation is based on the number of iteration of the simulation done. But the relationship between iterations and precision depends, also, on the precision of other the

variables used in the simulation program. In addition, the analyst must decide what degree of precision is required. It is important to taken into consideration that large numbers of simulator photons means more runtime.

3.3.2 Number of energy intervals

This parameter represents the number of intervals used to describe the range of photon energy spectrum. Figure (3.4) presents the effect of standard deviation of buildup factor as a function of iteration number.

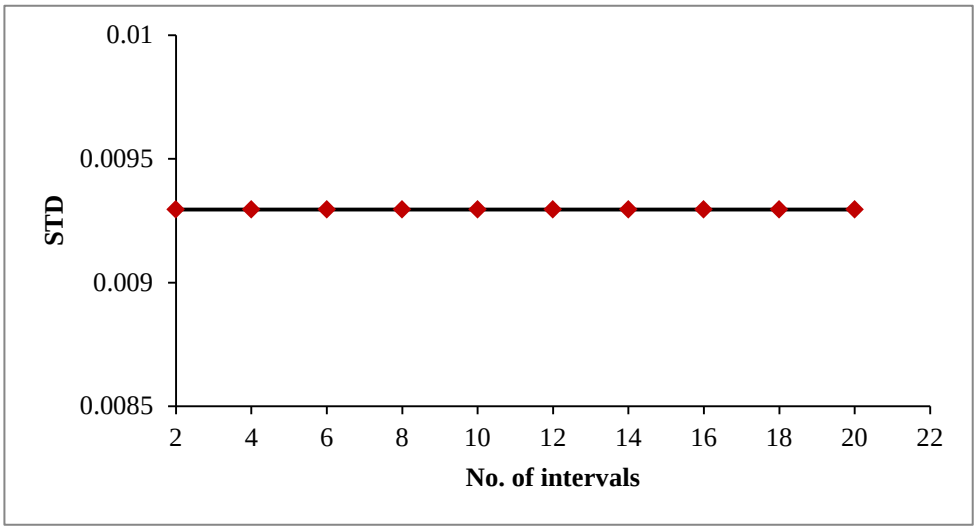

Fig (3.4) The effect of standard deviation as a function of interval number

It is obvious from figure (3.4) that there is no variation in standard deviation of the simulated buildup factor when the interval number increased or decreased. As a result the interval value is set 12 and considered as fixed parameter in all tests whose results are presented in this work.

3.4 Simulation Program Test Run

Before we start to study the effect of physical parameters, a preliminary test run for the simulation program was done to calculate the gamma ray buildup factor for Lead layer with a thicknesses (1 - 5) mfp and for energy 1 MeV and 10 MeV.

The energy value 10 MeV means that the pair production effect plays an important role in gamma ray interaction. For this reason we expect that the result of gamma ray buildup factor will be affected accordingly. The results of calculating the buildup for thickness and energy mentioned above are tabulated in table (3.5)

Table (3.5) Buildup factors with and without pair production for Pb at energy 1MeVand 10MeV

	E= 1MeV		E=10MeV	
Thickness mfp	B with pair production	B without pair production	B with pair production	B without pair production
1	1.35	1.35	1.189	1.089
1.5	1.488	1.488	1.261	1.134
2	1.609	1.609	1.327	1.215
2.5	1.77	1.77	1.401	1.326
3	1.829	1.829	1.589	1.360
3.5	1.935	1.935	1.639	1.442
4	1.887	1.887	1.779	1.518
4.5	2.027	2.027	1.879	1.623
5	2.043	2.043	1.980	1.724

Figures (3.5 A and B) show the relation between buildup factor as a function of Lead thickness for energy the two cases (1 MeV and 10 MeV), respectively. From table (3.4) and figure (3.5) we can conclude the following remarks:

1. There is no effect for pair production interaction on the calculation of buildup factor in the energy 1MeV. This result agree with the theoretical fact discussed before and this can be noticed in figure (3.5 A).
2. The effect of pair production on the calculation of buildup factor is very clear in the energy 10MeV. Since the values of buildup factor when we take the effect of pair production interaction are greater than the value of buildup factor in the absence of pair production interaction, and this can be noticed in figure (3.5 B). This result also agrees with the published result that will be studied analyzed and discussed later.

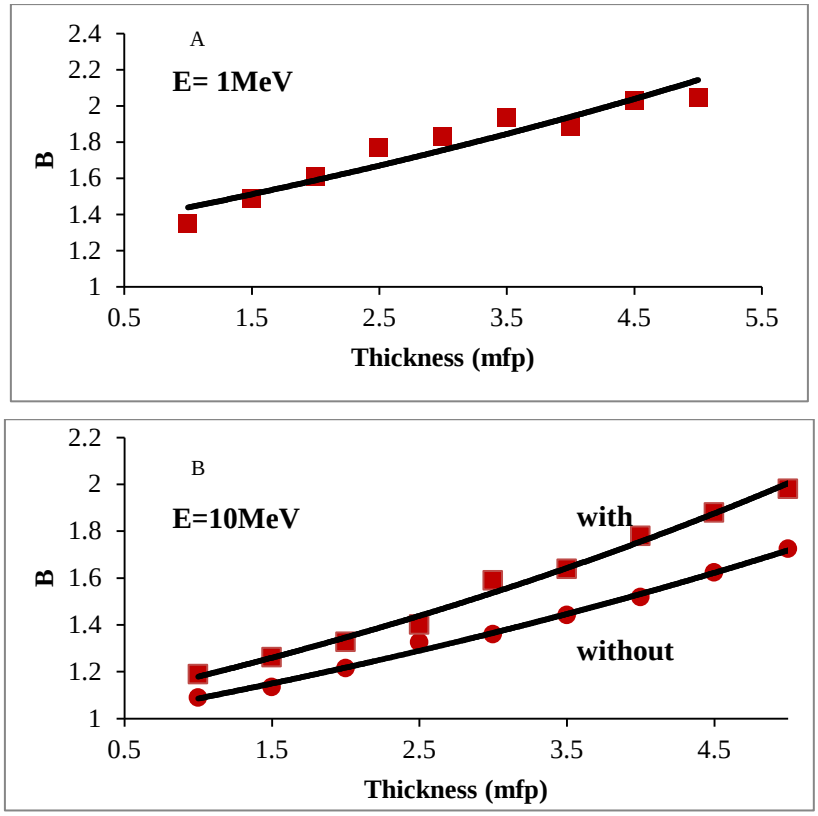

Fig (3.5) Buildup factor for Pb shield layer for the cases (A) 1MeV and (B) 10MeV

3.5 The Effect of Physical Parameters on Buildup Factor

The following parameters affect the value of buildup factor.

3.5.1 Thickness effect

To study the effect of the material thickness, the three materials aluminum, iron and lead were selected, individually, as shield material to investigate thickness effect. The values of buildup factor for different thickness values 1 - 5 mfp and for the three selected materials aluminum, iron and lead are presented in tables (3.6), (3.7) and (3.8) respectively.

Table (3.6) The effect of thickness on Buildup factor of Al layer for different energy values

Thickness in mfp	Buildup factor			
	4MeV	6MeV	8MeV	10MeV
1	1.481 ± 0.0085	1.473 ± 0.0090	1.424 ± 0.0091	1.41 ± 0.0095
1.5	1.742 ± 0.0138	1.719 ± 0.0144	1.657 ± 0.0151	1.62 ± 0.0153
2	2.05 ± 0.0208	1.97 ± 0.0217	1.911 ± 0.0224	1.906 ± 0.0234
2.5	2.329 ± 0.0305	2.249 ± 0.0316	2.164 ± 0.0330	2.174 ± 0.0342
3	2.605 ± 0.0427	2.507 ± 0.444	2.427 ± 0.0464	2.44 ± 0.0485
3.5	2.874 ± 0.0582	2.89 ± 0.0638	2.819 ± 0.0663	2.79 ± 0.0689
4	3.222 ± 0.0802	3.249 ± 0.0887	3.073 ± 0.0925	3.173 ± 0.0987
4.5	3.556 ± 0.1103	3.493 ± 0.1201	3.521 ± 0.1291	3.692 ± 0.1401
5	3.932 ± 0.1498	4.091 ± 0.1861	3.804 ± 0.1745	4.04 ± 0.1928

Table (3.7) The effect of thickness on Buildup factor of Fe layer for different energy values

Thickness in mfp	Buildup factor			
	4MeV	6MeV	8MeV	10MeV
1	1.458 ± 0.0084	1.361 ± 0.0085	1.312 ± 0.0087	1.254 ± 0.0089
1.5	1.687 ± 0.0133	1.558 ± 0.0135	1.491 ± 0.0138	1.416 ± 0.0138
2	1.934 ± 0.0200	1.742 ± 0.0199	1.657 ± 0.0199	1.571 ± 0.0201
2.5	2.123 ± 0.0284	1.964 ± 0.0280	1.817 ± 0.0279	1.683 ± 0.0279
3	2.363 ± 0.0399	2.167 ± 0.0389	2.028 ± 0.0388	1.866 ± 0.0386
3.5	2.713 ± 0.0552	2.35 ± 0.0531	2.177 ± 0.0527	2.029 ± 0.0524
4	2.995 ± 0.0759	2.597 ± 0.0720	2.454 ± 0.0725	2.27 ± 0.0704
4.5	3.232 ± 0.1020	2.894 ± 0.1004	2.641 ± 0.0985	2.46 ± 0.0969
5	3.68 ± 0.1415	3.045 ± 0.1301	2.862 ± 0.1321	2.564 ± 0.1260

Table (3.8) The effect of thickness on Buildup factor of Pb layer for different energy values

Thickness in mfp	Buildup factor			
	4MeV	6MeV	8MeV	10MeV
1	1.301 ± 0.0086	1.228 ± 0.0089	1.210 ± 0.0091	1.189 ± 0.0092
1.5	1.441 ± 0.0134	1.338 ± 0.0138	1.313 ± 0.0138	1.261 ± 0.0139
2	1.576 ± 0.0193	1.45 ± 0.0193	1.402 ± 0.0197	1.327 ± 0.0197
2.5	1.687 ± 0.0276	1.557 ± 0.0268	1.528 ± 0.0275	1.401 ± 0.0271
3	1.835 ± 0.0367	1.723 ± 0.0371	1.623 ± 0.373	1.589 ± 0.0381
3.5	1.966 ± 0.0491	1.815 ± 0.0492	1.717 ± 0.0498	1.639 ± 0.0505
4	2.119 ± 0.0655	1.935 ± 0.0660	1.852 ± 0.0678	1.779 ± 0.0682
4.5	2.316 ± 0.0895	2.08 ± 0.0881	2.010 ± 0.0911	1.879 ± 0.0908
5	2.540 ± 0.1198	2.445 ± 0.124	1.954 ± 0.1147	1.980 ± 0.1206

Figures (3.6), (3.7) and (3.8) show the relation between buildup factor and thickness for aluminum, iron and lead, respectively. The range of thickness for these material was taken 1 - 5 mfp, the simulation was conducted for the energy case 4, 6, 8 and 10 MeV.

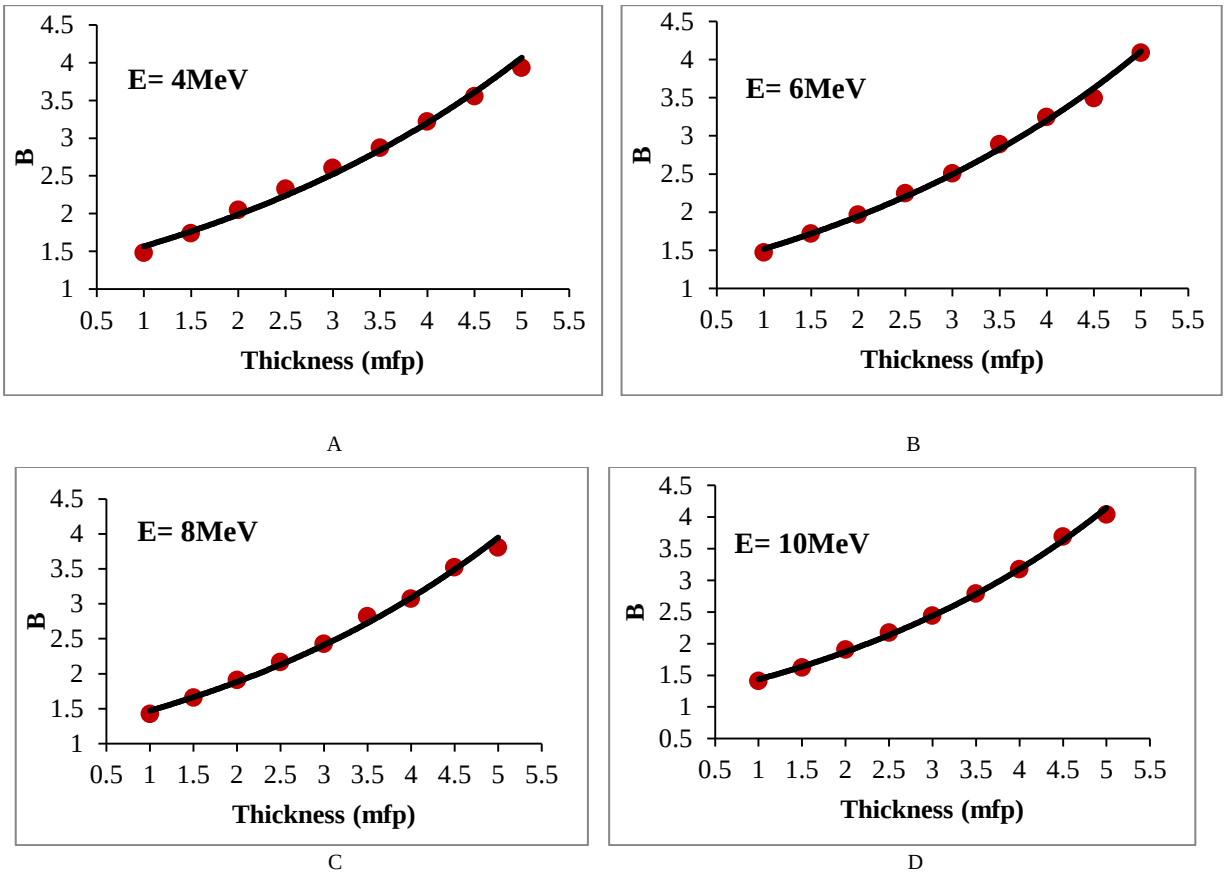

Fig (3.6) The relation between Buildup factor and thickness for Al layer at energy (A) 4MeV (B) 6MeV, (C) 8MeV,and (D) 10MeV

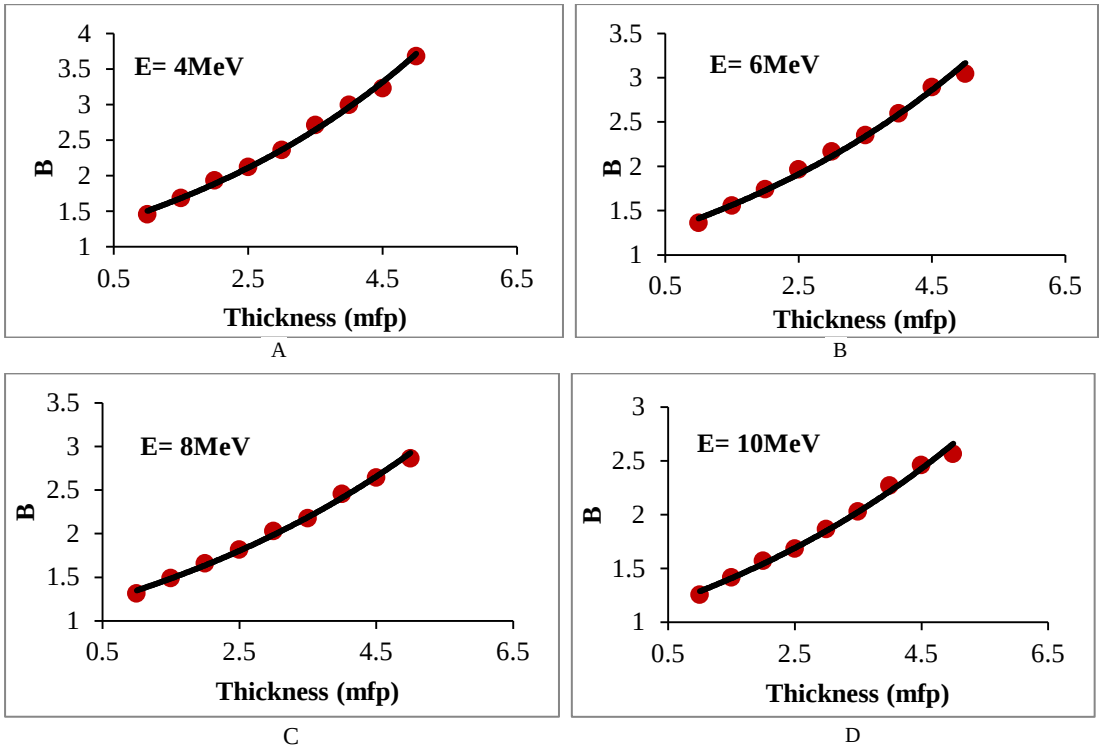

Fig (3.7) The relation between Buildup factor and thickness for Fe layer at energy (A) 4MeV (B) 6MeV (C) 8MeV (D) 10MeV

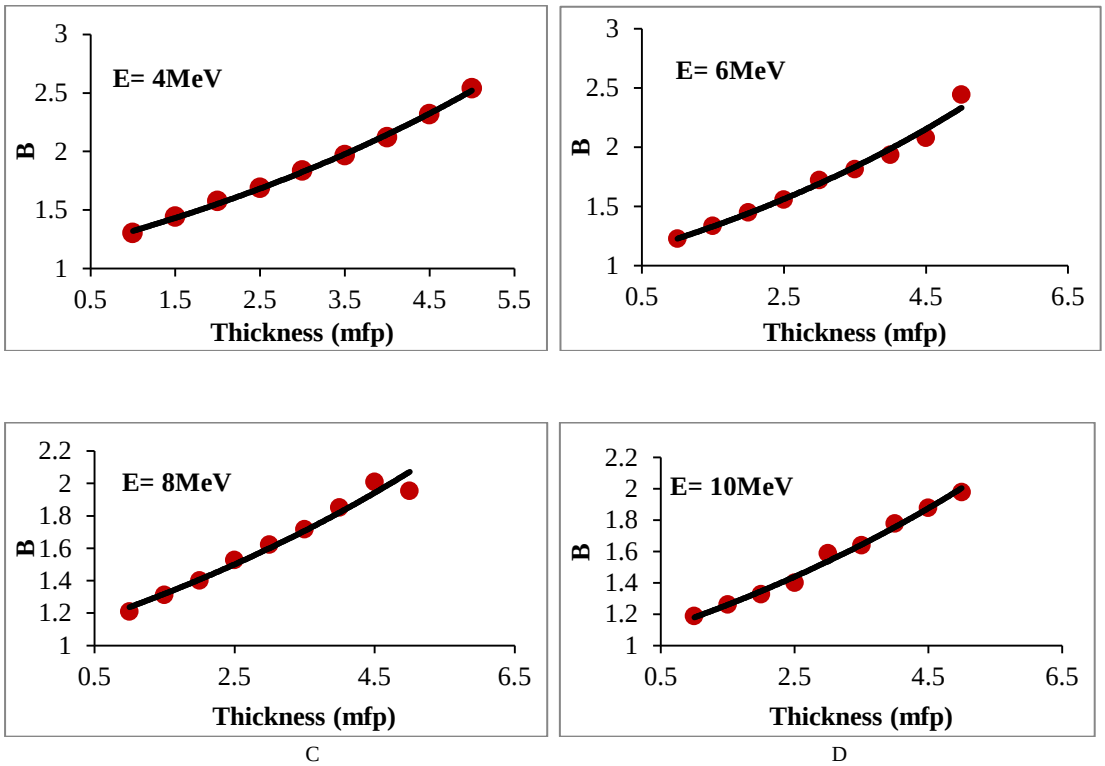

Fig (3.8) The relation between Buildup factor and thickness for Pb layer at energy (A) 4MeV (B) 6MeV (C) 8MeV (D) 10MeV

From the above figures (3.6), (3.7) and (3.8), one can conclude that gamma ray buildup factor increases with the increase of shield thickness for all the types of selected shielding material under this study. The increase of buildup factor is due to the increase of scattering with the small angles when the shield thickness is increased.

3.5.2 Atomic number effect

The effect of atomic number on gamma ray buildup factor was investigated in this study. A set of tests were conducted to study of effect of Z on buildup factor; and for the shielding materials aluminum (Z = 13), iron (Z = 26) and lead (82) and for the energy 10MeV. Table (3.9) presents the values of buildup factor for the three mentioned materials.

Table (3.9) Buildup factor for Al, Fe and Pb at energy case 10 MeV

E= 10MeV			
Thickness in mfp	Buildup factor		
	Al	Fe	Pb
1	1.41 ± 0.0095	1.254 ± 0.0089	1.189 ± 0.0092
1.5	1.62 ± 0.0153	1.416 ± 0.0138	1.261 ± 0.0139
2	1.906 ± 0.0234	1.571 ± 0.0201	1.327 ± 0.0197
2.5	2.174 ± 0.0342	1.683 ± 0.0279	1.401 ± 0.0271
3	2.44 ± 0.0485	1.866 ± 0.0386	1.589 ± 0.0381
3.5	2.79 ± 0.0689	2.029 ± 0.0524	1.639 ± 0.0505
4	3.173 ± 0.0987	2.27 ± 0.0704	1.779 ± 0.0682
4.5	3.692 ± 0.1401	2.46 ± 0.0969	1.879 ± 0.0908
5	4.04 ± 0.1928	2.564 ± 0.1260	1.980 ± 0.1206

From figure (3.9) it is clear that the buildup factor for low atomic number material, (Al, Z=13), is higher than that for medium (Fe, Z=26) and heavy (Pb, Z=82) materials at the energy (10 MeV). A rapid decrease of the buildup factor values with increasing the Z is notice. This dependence and by returning to table (3.2) and (3.3) is in a good agreement with the fact that the proportion of the cross section for Compton effect decreases with increase of atomic number, therefore the Compton effect plays a more significant role in lighter materials that having lower atomic number (Z).

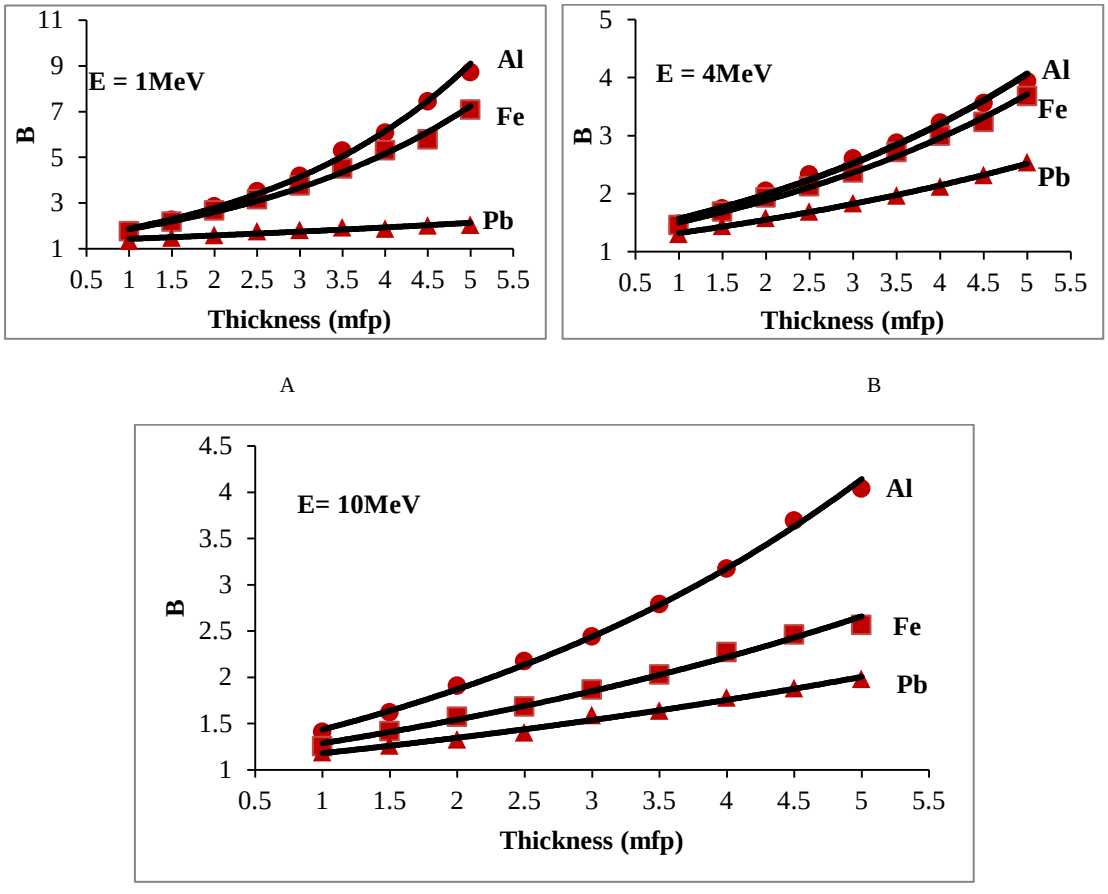

Fig (3.9) Dependence of Buildup factor on thickness of the material layer for Al, Fe and Pb

3.5.3 Energy effect

To study the effect of initial photon energy on the calculation of gamma ray buildup factor, four initial energy values 4, 6, 8 and 10 MeV were applied for the three selected shielding materials and for thicknesses up to 5 mfp. This range of energy was chosen to ensure that the effect of pair production was included in the simulation calculations, and this is one of the most important goals in this study.

The test results are shown in tables (3.6), (3.7) and (3.8), and figures (3.10), (3.11) and (3.12) for Al, Fe and Pb, respectively. The results indicated that the gamma ray buildup factor is inversely proportional with energy increase. Within the studied energy range (4 - 10) MeV this act was noticed for the three materials studied in this research and within the range of energy (4 - 10) MeV. This behavior can be explained that "when the energy is increased, the penetrating ability for gamma ray is also increase and this, in turn, leading to an increase in the probability of scattering, and finally it is reflected on the buildup value, since scattering plays an important role in increasing buildup factor".

The results shown in figures (3.10), (3.11) and (3.12), also, indicates that the rate of increase in the values of buildup factor of Pb is rather than for Fe and the last is more than for Al. This is due to the effect of interaction of the pair production; which is directly proportional with the atomic number square (as be mentioned in chapter one).

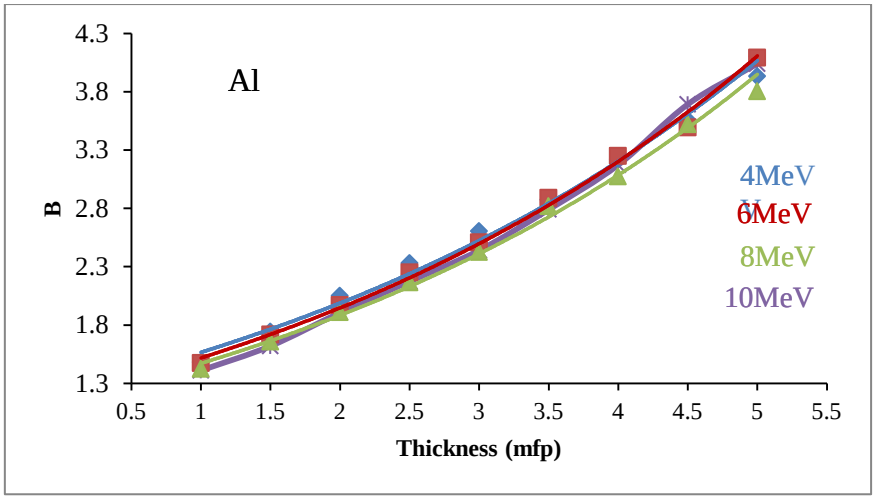

Fig (3.10) Effect of source energy on Buildup factor for Al layer

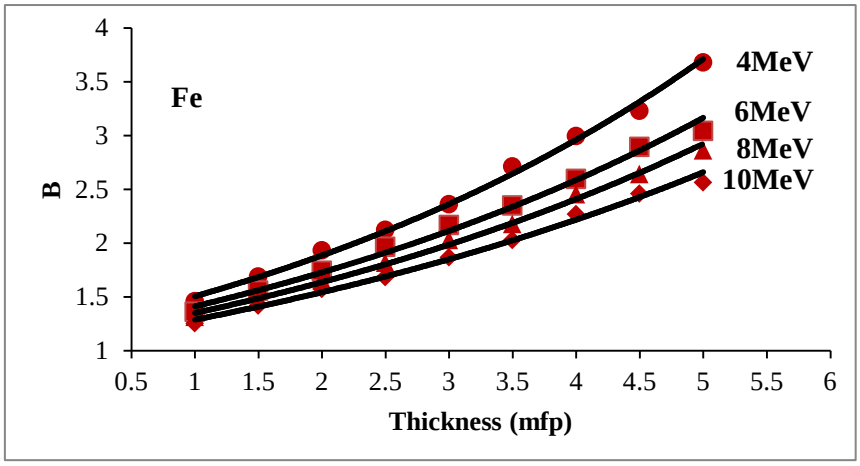

Fig (3.11) Effect of source energy on Buildup factor for Fe layer

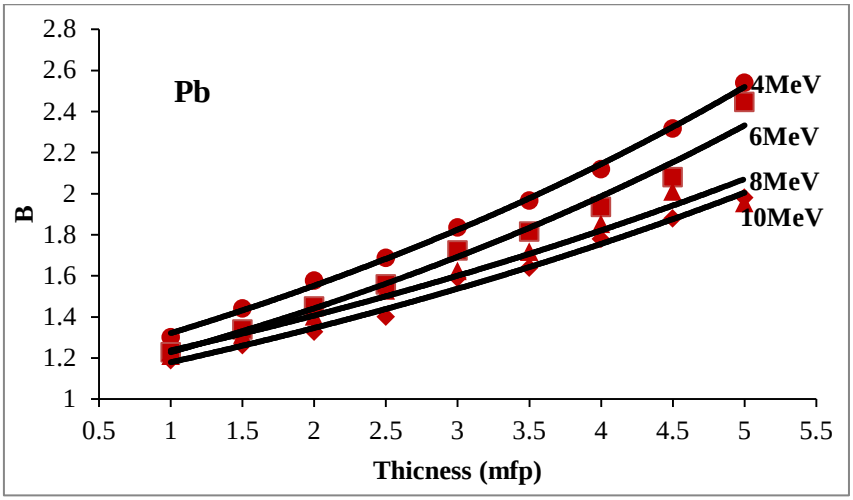

Fig (3.12) Effect of source energy on Buildup factor for Pb layer

3.6 Buildup factor in the Presence and Absence of Pair Production

To investigate the differences between gamma ray buildup factor values in the absence and presence the effect of pair production, the simulated program was executed in the absence of pair production effect (i.e., considering the effect of Compton scattering only). This test is accomplished by ignoring the pair production effect, at first, and keeping the occurrence of Compton effect only. Then as second test both types of interactions are taken into consideration.

In the two cases, the program was executed for the three chosen material (Al, Fe and Pb) and for the energy range (4 - 10) MeV and for thickness up 5mfp. From figures (3.13), (3.14) and (3.15) it is clear that the calculated values of buildup in the presence of pair production are higher than the calculated value of buildup factor in case of ignorance of pair production events.

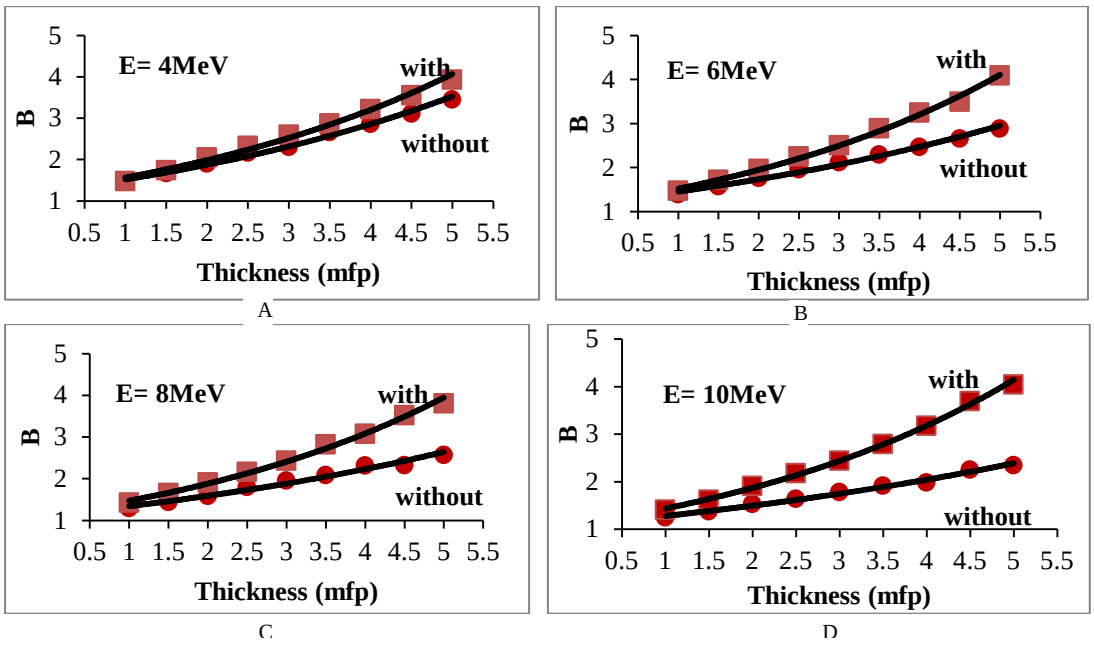

Fig (3.13) The Buildup factor with and without effect of pair production, for Al layer when the source energy is (A) 4MeV (B) 6MeV (C) 8MeV and (D) 10MeV

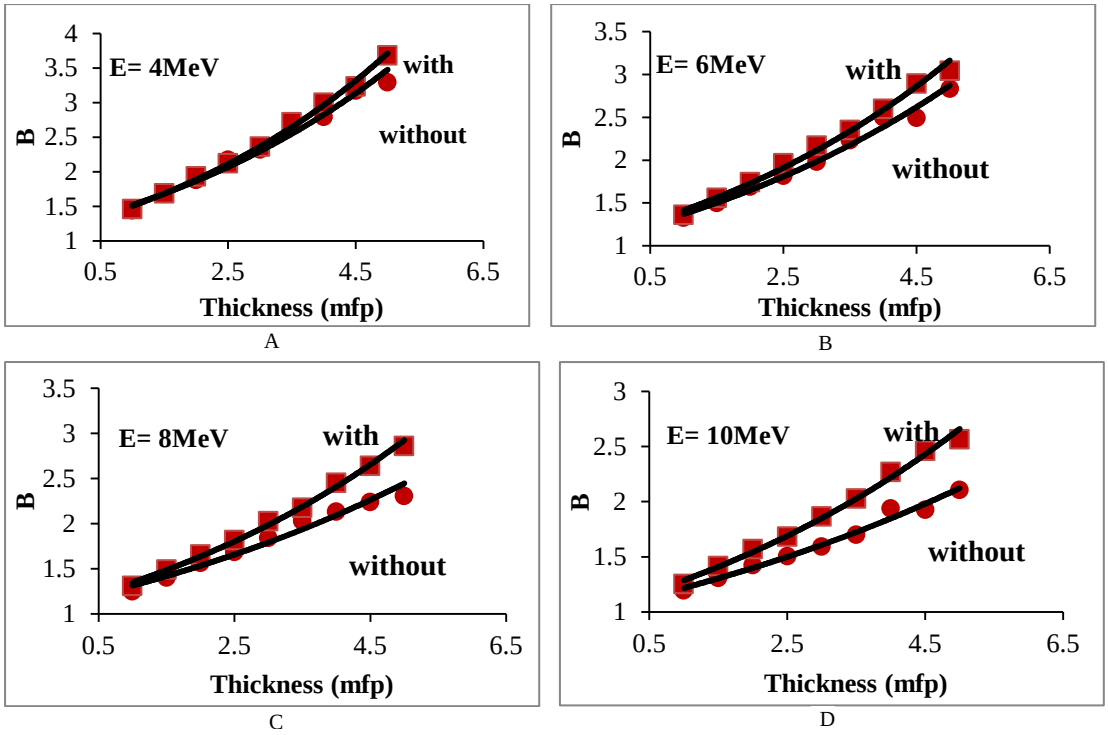

Fig (3.14) The Buildup factor with and without effect of pair production for Fe layer when the source energy is (A) 4MeV (B) 6MeV (C) 8MeV and (D) 10MeV

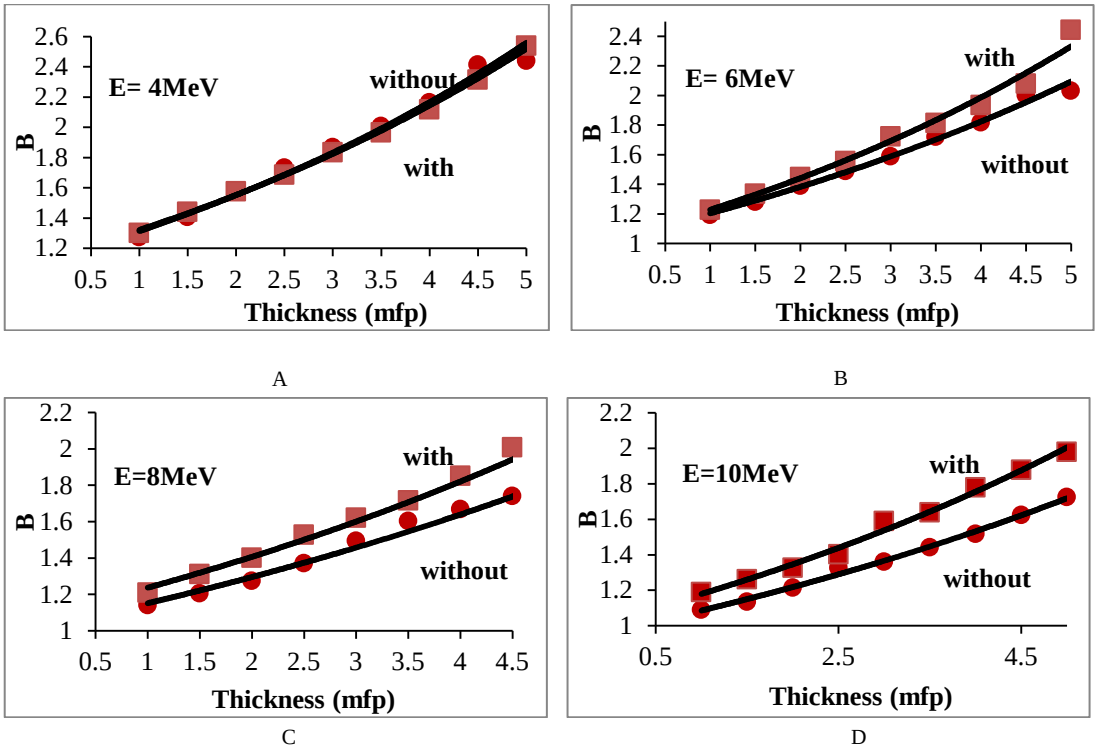

Fig (3.15) The Buildup factor with and without effect of pair production for Pb layer when the source energy is (A) 4MeV (B) 6MeV (C) 8MeV and (D) 10MeV

This means that the contribution the pair production interaction causes an increase in the value of buildup factor. We can also notice from these figures that the deviation between the two curves (with and without the effect of pair production) is increased when the source energy is increased within the studied energy range (4 - 10) MeV and for all the three chosen material up to 5 mfp thickness. We can interpret these results by returning to table (3.3) which shows that the cross section for pair production is increased when the energy is increased (within the studied energy range).

The ratio between gamma ray buildup factor in case of with and without pair production effect as a function of material thickness for Al, Fe, and Pb for energy (4, 6, 8 and 10) MeV are demonstrated in figure (3.16). It’s clear from this figure that the deviation from the Base line is increased with increase of source energy for all the studied material. Also, we can note from this figure that this deviation, more rapidly increased when the atomic number decreased.

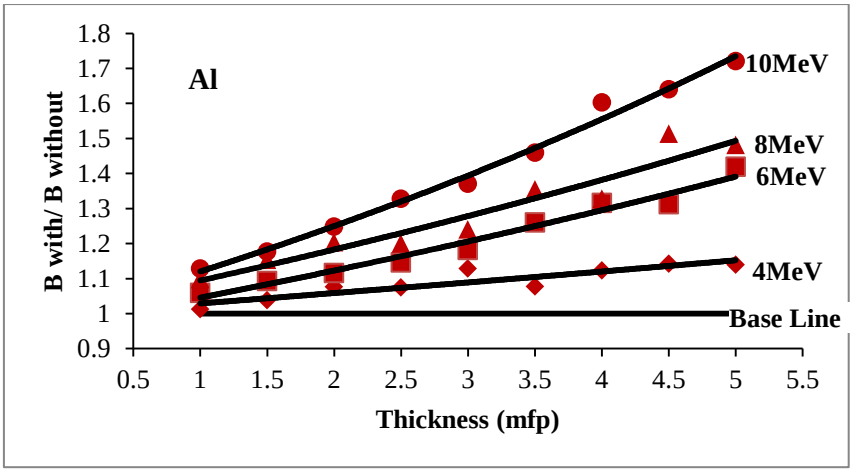

A

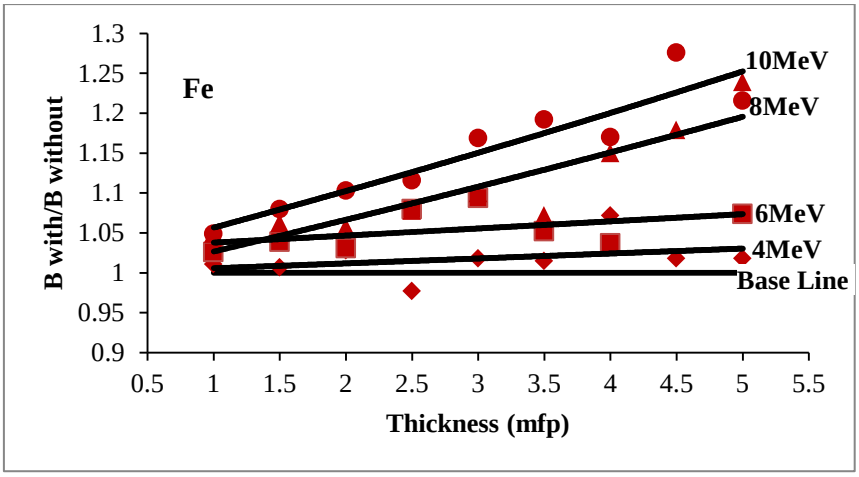

B

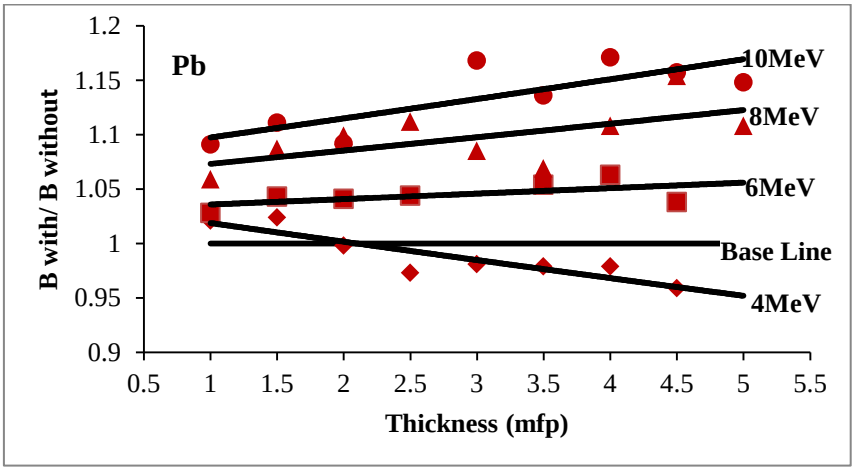

C

Fig (3.16) The ratio between gamma ray buildup factor in case with and without pair production effect as a function of material thickness for (A) Al, (B) Fe and (C) Pb

Chapter Four
Summary, Conclusions and Suggestions

4.1 Summary

In this thesis project, a computer program was designed and implemented to calculate dose buildup factor for aluminum, iron and lead at the source energy range 4 – 10 MeV and thickness 1 - 5 mfp. This program is designed based on Monte Carlo method through simulating the main gamma ray interaction with the matter which affect on dose build up factor calculation. The considered gamma interactions in the developed program are Compton scattering and pair production.

4.2 Conclusions

Throughout this study and the yielded results, the following remarks are concluded:

- Dose buildup factor increased with increase of thickness for all types of the selected shielding material under study. The increase in the value of dose buildup factor is due to the increase of gamma scattering with small angles and increase of shield thickness.
- Dose buildup factor for low atomic number material (Al, Z=13) is higher than that for medium (Fe, Z=26) and heavy (Pb, Z=82) materials within the studied energy range (4-10MeV). A rapid decrease of the buildup factor values with increase of Z was noticed. This dependence is in good agreement with the fact that the cross section for Compton scattering decreases with increase of atomic number. The effect of Compton scattering plays significant role in lighter materials.
- Gamma ray buildup factor is inversely proportional with increase of energy within the studied energy range (4 - 10) MeV. This is due to the

increase of cross section for pair production interaction with the energy, within the studied energy, mean while the cross section for Compton scattering decreases rapidly with increase of energy and, consequently the probability of scattering is decreased and thus behavior is finally reflected on the buildup calculation.

The results show that the rate of increase (i.e., the variation or the deviation from energy to energy) in the values of buildup factor for Pb shield is greater than that for Fe and the last more than Al. This is due to the effect of the interaction of the pair production which is directly proportional with square of the atomic number.

- The calculated values of buildup in the presence of pair production are higher than the calculated value of buildup factor in the absence of pair production interaction effect. This is due to the increases in pair production effect. The contribution of pair production is increased when the energy is increased within the studied energy range (4 - 10) MeV compared with the contribution of Compton scattering for all studied material. This is so because the cross section for pair production is increased when the energy is increased within the studied energy range.

4.3 Suggestions for Future Works

1. Modify the simulation program to be capable for studying the buildup factor for multi layers including the effect of pair production event.
2. Study the effect of pair production on buildup factor for materials have low atomic number.
3. Study the behavior of buildup factor including effect of pair production for high energy, higher than 10 MeV.
4. Study the effect of source geometry (point, spherical and cylindrical) one buildup factor calculations.

References

[Al-Am 96]

Al-Ammar, H.; "Studying the Buildup Factor and Angular Distribution of Gamma Rays in Multi-Layer Shields", College of Science, Baghdad University, (M. Sc.Thesis), (1996).

[Alam 11]

Alamatsaz, M. H. and Mokari, M.; "Calculating gamma ray exposure buildup factors for plane source and double stratified layers of water and lead and investigating effect of coherent scattering on these factors", Iranian Journal of Physics Research, Vol.10,No.4,(2011), P.295-300.

[Al-An 89]

Al-Ani, L.; "Study of the Buildup Factor in Different Material", College of Science, Baghdad University, M. Sc.Thesis, (1989).

[Al-An 06]

Al-Ansari, M.; "Simulation of Buildup Factor for Bremsstrahlung Produced by Complete Absorption of Beta Rays", College of Science, Al-Nahrain University, M.sc. Thesis, (2006).

[Al-Ba 01]

Al-Baiti, K.; "Measurement and Calculation of Gamma Ray Buildup Factor in Single and Multi-Layer Shields", College of Science, University of Babylon, M. Sc.Thesis, (2001).

[Al-Sa 02]

Al-Samaraey, Anwer; "Calculation of Gamma Rays Buildup Factor for the Conical Beam Using Monte Carlo Method", College of Science, Baghdad University, M. Sc. Thesis, (2002).

[Al-Ra 03]

Al-Rawi, A.; "Monte Carlo Method Calculation for Buildup Factor in Different Materials", College of Science, Al-Nahrain University, M. Sc.Thesis, (2003).

[Bako 94]

Bakos, G.C.; "Photon Penteration through Thick Double-Layer Shielding Slabs", Ann. Nucl. Eng., Vol.21,(1994), P.651.

[Bhat 67]

Bhattacharya, P. K.; "Estimation of a probability density function and its derivatives ", The Indian Journal of Statistic, Vol.29, No.4, (1967), Pp.373-382.

[Bind 79]

Binder, Dr. Kurt; "Monte Carlo Methods in Statistical Physics", Springer-Verlag Berlin Heidelberg, New York, (1979).

[Bish 87]

Bishop, G.B.; "Penetration of 2.75 MeV γ-Rays Through Shielding Slabs of Graphite, Al, Steel and Pb", Nucl. Ins. Meth. Vol.225, (1987), P.165.

[Brod 62]

Broder, D. L.; "The Use of Multigroup Methods in Bilogical Shielding calculations" Soviet J. of Atomic Energy, Vol.12, (1962), P.30.

[Burk 74]

Burke, G.P. and Beck, H.L.; "Calculated and Measured Dose Buildup Factors for Gamma Rays Penterating Multi-layered Slabs", Nucl. Sci. and Eng., Vol.53, (1974), Pp.109-112.

[Buch 92]

Buchanan, James L.;"Numerical Method and Analysis", McGraw-Hill, Inc., 1992.

[Capo 58]

Capo, M. A.; "Polynomial Approximation of Gamma Ray Buildup Factors for Point Isotropic Source", Appex-510, 1958.

[Chil 84]

Chilton, A.B.; "Principles of Radiation Shielding"; Prentice Hall, Inc., London, 1984.

[Chil 80]

Chilton, A. B., Eisenhauer, C. M. and Simmons, G. L.; "Photon Point Source Buildup Factors for Air, Water and Iron" Nucl. Sci. and Eng., Vol.73, (1980), P.97.

[Dhil 12]

Dhillon, J. S. and Singh, B. and Sidhu, G. S.; "Gamma Ray Phpton Energy Absorption Buildup Factor Study In Some Soils" IOSR Journal of Applied Physics, 2278-4861 Vol.1, Issue 6, (2012), P14-21.

[Eise 75]

Eisenhaure, C.M. and Simmon, G.L.; "Point Isotropic Gamma Ray Buildup Factor in Concrete", Nucl. Sci. and Eng. Vol.56, (1975), P.263.

[Evan 55]

Evans, Ropley D.; "The Atomic Nucleus", McGraw-Hill, Inc. Printed in the United State of America, 1955.

[Fish 86]

Fisher, Diana; "Advanced Basic "; Computer Science Press, 1986.

[Fode 81]

Foderaro, A. and Hall, R. J.; "Application of three Exponential Representation of Photon Buildup Factors to Water", Nucl. Sci. and Eng. Vol.78, No.1, (1981), Pp.74-78.

[Fong 89]

Fong, Min-Su and Jiang, Shiang-Huei; "Gamma Ray Buildup Factors for a Point Isotropic Source in Stratified Spherical Shields", Nucl. Sci. and Eng., Vol.102, (1989), P.64.

[Gold 54]

Goldstein, H. and Wilkins,J. E.; "Calculation of the Penetration of Gamma Ray", U.S.Atomic energy Comission, NYO-3075,1954.

[Gold 59]

Goldstein, H. ; "Fundamental Aspects of Reactor Shielding", Addison-Wesley Publishing, Inc. London, 1959.

[Hamm 64]

Hammersley, J. M. and Handscomb, D. C.; “Monte Carlo Methods”, Fletcher and Son Ltd, Norwich, 1964.

[Hatt 94]

Hattif, K.; "Gamma Ray Buildup Factor Measurement in Different Material", College of Science, Baghdad University, Ph.D. thesis, 1994.

[Herb 88]

Herbold, G.; "Monte Carlo Calculation if Energy Buildup Factors in the Range from 15 keV to 100 keV, with Special Reference to the Dosimetry of ^{125}I Seeds", Nucl. Tech., Vol.33, No.9, (1988), P.1037.

[Hira 87]

Hirayama, H.; "Exposure Buildup Factors of High Energy Gamma Rays for Water, Concrete, Iron and Lead", Nucl.Tech., Vol.77, (1987), Pp.60-67.

[Hubb 63]

Hubbell, J. H.; "A Power Series Buildup Factor Formulation. Application to Regtangular and off-Axis Disk Source Problems", Journal of research of the National Bureau of Standards-C. Engineering and Instrumentation, 67C, P.291-306, 1963.

[Jian 80]

Jiang, Shiang-Huei; "Gamma Ray Buildup Factors for Stratified Lead and Water Shields", Nucl. Sci. and Eng., Vol.75, P.16, 1980.

[Kado 98]

Kadotani, H. and Shimizu, A.; "Gamma Ray Albedo Data Generated by the Invariant Embedding Method", J. Nucl. Sci. Tech., Vol.35, P.584, 1998.

[Kapl 77]

Kablan, Irving; "Nuclear Physics", Adisson-Weseley publishing company. Inc., 1977.

[Khan 84]

Khan, Fiaz M.; "Physics of Radiation Theraby", Wlliams and Wilkins, 1984.

[Knol 00]

Knoll, G. F.; "Radiation Detection Measurement", 3rd edition, University of Michigan, John Wiley and Sons, Ltd, 2000.

[Knol 79]

Knoll, G. F.; "Radiation Detection and Measurement"**,** John Wiley and Sons, New York, 1979.

[Kran 88]

Krane, S. K.; "Introductory Nuclear Physict", 2nd edition, Oregon State University, John Wiley and Sons, 1988.

[Makk 09]

Makki, H.; "Computational Study for Gamma Rays Buildup Factor for Multi-Layer Slab Shield in Finite Media", College of Science, Baghdad University, M.Sc. Thesis, 2009.

[Mano 10]

Manohara, S.R., Hanagodimath, S. M. and Gerward, L.; "Energy Absorption Buildup Factors for Thermoluminescent Dosimetric Materials and their Tissue Equivalence", Radiation Physics and Chemistry, Vol.79, Iss.5, (2010), Pp.575-582.

[Metg 78]

Metghalchi, Mahmoud; "Berger Coefficients for the Eisenhauer-Simmons Gamma Ray Buildup Factors in Ordinary Concrete", Nucl. Sci. and Eng., Vol.67, P.341, 1978.

[Meye 67]

Meyerhof, W. E.; "Elements of Nuclear Physics", MCGRAW Hill, New Yourk, 1967.

[Morr 75]

Morris, E. E., Chilton, A. B. and Vetter, A. F.; "Tabulation and Empirical Representation of Infinite Medium Gamma Ray Buildup Factors for Monoenergetic, Point Isotropic Sources in Water, Aluminum and Concrete", Nucl. Sci. and Eng., Vol.56, (1975), Pp.171-178.

[Morr 70]

Morris, E. E. and Chilton, A. B.; " Buildup Factors in Water for Gamma Rays at 1 MeV and Lower Energy", Nucl. Sci. and Eng., Vol.40, (1970), Pp.128-152.

[Nayl 66]

Naylor, T. J., Balintfy, J. L., Burdick, D. S. and Chu, K.; "Computer Simulation Techniques", Wiley, New York, 1966.

[Ochb 12]

Ochbclagh, D. and Azimkhani, S.; "Investigation of Gamma Ray Shielding Properties of Concrete Containing Different Percentages of Lead", Applied Radiation and Isotopes, Vol.70, Iss.10, (2012), Pp.2282-2286.

[Rubi 81]

Rubinstein, R. Y.; "Simulation and the Monte Carlo methods", John Wiley & Sons, New York, 1981.

[Sard 09]

Sardari, D., Abbaspour, A., Baradaran, S. and Babapour, F.; "Estimation of Gamma and X-ray Photons Buildup Factors in Soft tissue with Monte Carlo Method", Applied Radiation and Isotopes, Vol.67, Iss.7-8, (2009), Pp.1438-1440.

[Shim 00]

Shimizu, A.; "Development of Angular Eigen Value Method for Radiation Transport Problems is Slabes and Its Application to Penteration of Gamma rays", Nucl. Sci. Tech., Vol.37, (2000), Pp.15-25.

[Shim 02]

Shimizu, A.; "Calculation of Gamma rays Buildup Factors up to Depth of 100 mfp by the Method of Invariant Embedding (I)" Nucl. Sci. Tech., Vol.39, No.5, (2002), P.477.

[Shir 13]

Shirani, A. and Alamatsaz, M. H.; "Calculation of exposure buildup factors for point isotropic gamma ray sources in stratified spherical shields of water surrounded by lead and optimization of water-lead combination", Iranian Journal of Science and Technology, IJST, A1:Vol.29, (2013), 34.

[Sing 12]

Singh, B., Dhillon, J. S. and Sidhu, G. S.; "Gamma Ray Photon Exposure Buildup Factores in Some Fly Ash:A Study", International Journal of Scientific and Research Publications, Vol.2, Iss.9,(2012).

[Span 69]

Spanier, Jerome, and Gelband, Ely M.; "Monte Carlo Principles and Neutron Transport Problems", Addison-Wesley Publishing Co. 1969.

[Whit 50]

White, G. R.; "The Penetration and Diffusion of Co^{60} Gamma Ray in Water Using Spherical Geometry", Phys. Rev., Vol.80, P.154, 1950.

[Wood 81]

Wood, J.; "Computational Methods in Reactor Shielding", Perogamon Press, U.K, 1981.

[Xcom]

http:// Physics.nist.gov/PhysRefData/Xcom/htm1/Xcom1.htm1.

الخلاصة

تم تصميم وكتابة برنامج حاسوبي باعتماد طريقة مونتي كارلو باستخدام لغة بيسك المرئية (الاصدار G) حيث وضفت هذه الطريقة لمحاكاة المسألة التقليدية (الكلاسيكية) في سقوط حزمة اشعة كاما على شريحة مستوية تعمل كمادة موهنة لاشعة كاما. ان الشكل الهندسي للمصدر المشع الذي تم اعتماده في هذه الدراسة وتوظيفه في بناء البرنامج هو المصدر العمودي المستوي.

في هذا البحث تم حساب عامل تراكم الجرعة لفوتونات كاما بوجود وعدم وجود تاثير انتاج الزوج ضمن مدى الطاقة ١٠-٤ م.أ.ف لكل من الالمنيوم والحديد والرصاص ولغاية سمك ٥ معدل مسار حر.

كما تم في هذا البحث دراسة تأثير بعض العوامل الفيزياوية المتعلقة بالدروع وقد اظهرت نتائج المحاكاة النقاط الاتية:

ان عامل تراكم اشعة كاما يزداد بزيادة سمك مادة التدريع وللمواد الثلاثة المدروسة، وقد تم تفسير هذه الزيادة في عامل تراكم الجرعة الى زيادة احتمالية الاستطارة بزوايا صغيرة مع زيادة سمك مادة التدريع.

ان عامل تراكم الجرعة للمواد (الدروع) الخفيفة ذات العدد الذري القليل كما في الالمنيوم (Al, Z=13) يكون اعلى منها في المواد المتوسطة ذات العدد الذري المتوسط كما في الحديد (Fe, Z=26) والاخير يكون اعلى من المواد الثقيلة ذات العدد الذري العالي كما في الرصاص (Pb, Z=82) ولنفس الطاقة (١٠ م.أ.ف) حيث يمكن ملاحظة التناقص السريع في قيم عامل التراكم مع زيادة العدد الذريZ. هذه العلاقة تتفق بشكل جيد مع حقيقة ان المقطع العرضي لتاثير كومبتن يتناقص مع زيادة العدد الذري حيث ان تاثير كومبتن يلعب دورا مهما في المواد الخفيفة ذات الاعداد الذرية الواطئة.

ان عامل تراكم الجرعة يتناسب تناسب عكسي مع زيادة الطاقة ضمن مدى الطاقة المدروسة في هذا البحث (١٠-٤) م.أ.ف تم تفسير هذا التناسب في علاقة عامل التراكم مع الطاقة باعتبار ان المقطع العرضي لاستطارة كومبتن ضمن هذا المدى من الطاقة يتناقص بزيادة الطاقة وهذا يعني ان احتمالية الاستطارة سوف تتناقص والتي بدورها سوف تنعكس على حسابات عامل التراكم حيث ان الاستطارة لها دور كبير في زيادة عامل التراكم.

ان معدل الزيادة في قيم عامل تراكم الجرعة في الرصاص -٨٢ تكون اكبر مما عليه في الحديد -٢٦ والاخير يكون اكبر مما عليه في الالمنيوم-١٣ وهذا يعود الى ان تاثير تفاعل انتاج الزوج يتناسب طرديا مع مربع العدد الذري.

ان عامل تراكم الجرعه بوجود تاثير انتاج الزوج يكون اكبر من عامل تراكم الجرعه بغياب تاثير انتاج الزوج حيث وجد ان الانحراف في قيم عامل تراكم الجرعه بوجود وعدم وجود تاثير انتاج الزوج يزداد بزيادة الطاقة ضمن مدى الطاقة المدروس وذلك لان المقطع العرضي لانتاج الزوج يزداد ضمن هذا المدى من الطاقة.

جمهورية العراق
وزارة التعليم العالي والبحث العلمي
جامعة النهرين
كلية العلوم

محاكاة عامل تراكم الجرعة لأشعة كاما متضمناً تأثير أشعة الفناء للألمنيوم، والحديد والرصاص

رسالة مقدمة الى
كلية العلوم – جامعة النهرين
وهي جزء من متطلبات نيل درجة ماجستير علوم في الفيزياء
من قبل

مروة صباح مهدي

(بكالوريوس علوم في الفيزياء 2011)

بأشراف

د. ليث عبد العزيز العاني

د. لؤي أدور جورج

جمادى الاولى 1435

آذار 2014